PD-LJ-87-350R

physical dynamics, inc.

Primer on Beam Optics

Charles R. Eminhizer

The views, opinions, and findings contained in this document are those of the author and should not be construed as official Department of the Army position, policy or decision, unless so designated by other official documentation.

REPORT DOCUMENTATION PAGE		READ INSTRUCTIONS BEFORE COMPLETING FORM
1. REPORT NUMBER PD-LJ-87-350R	2. GOVT ACCESSION NO.	3. RECIPIENT'S CATALOG NUMBER
4. TITLE *(and Subtitle)* Primer on Beam Optics		5. TYPE OF REPORT & PERIOD COVERED Topical Report
		6. PERFORMING ORG. REPORT NUMBER PD-LJ-87-350R
7. AUTHOR(s) Charles R. Eminhizer		8. CONTRACT OR GRANT NUMBER(s) DASG60-86-C-0011 GRC Sub 955-86-24
9. PERFORMING ORGANIZATION NAME AND ADDRESS Physical Dynamics, Inc. P. O. Box 1883 La Jolla, California 92038		10. PROGRAM ELEMENT, PROJECT, TASK AREA & WORK UNIT NUMBERS
11. CONTROLLING OFFICE NAME AND ADDRESS U.S. Army Strategic Defense Command P. O. Box 1500 Huntsville, Alabama 35807		12. REPORT DATE
		13. NUMBER OF PAGES 108
14. MONITORING AGENCY NAME & ADDRESS(*If different from Controlling Office*)		15. SECURITY CLASS. *(of this report)* Unclassified
		15a. DECLASSIFICATION/DOWNGRADING SCHEDULE

16. DISTRIBUTION STATEMENT *(of this Report)*

Approved for public release, distribution unlimited.

17. DISTRIBUTION STATEMENT *(of the abstract entered in Block 20, if different from Report)*

18. SUPPLEMENTARY NOTES

19. KEY WORDS *(Continue on reverse side if necessary and identify by block number)*
Accelerator Design, Beam Optics, Beam Transport, Magnetic Optics.

20. ABSTRACT *(Continue on reverse side if necessary and identify by block number)*
This is a primer on beam optics with emphasis on neutral particle beam (NPB) optical devices. It explains how the motion of charged particles in magnetic and electric fields is calculated and how devices (primarily magnets) are designed, used and combined to make a beam transport system.

DD $_{1\ JAN\ 73}^{FORM}$ 1473

Primer on Beam Optics

Charles R. Eminhizer

Physical Dynamics, Inc.
San Diego, California

Table of Contents

i

Figures

Introduction

1.1 Organization of this Primer

This primer is intended as an introduction to beam optics with particular emphasis on neutral particle beam (NPB) optical devices. It explains how the motion of charged particles in magnetic and electric fields is calculated and how devices (primarily magnets) are designed, used and combined to make a beam transport system.

The design of a transport system such as that of an NPB device requires very sophisticated mathematical techniques and complicated computer codes. Technical reports and articles describing this process assume the reader has a graduate level knowledge of physics and applied mathematics including classical and relativistic dynamics, electromagnetic theory, statistical mechanics, differential equations, vector analysis, matrix algebra and Lie algebra. It is impossible to cover all relevant topics in this primer. If the reader is interested in a more thorough presentation of some of these topics, he is referred to an introduction book by Stanley Humphries, Jr. titled Principles of Charged Particle Accelerators, Ref. [1]. It presents topics in both particle acceleration and beam transport but is a long book, 555 pages.

Like all areas of science, considerable terminology and jargon has developed as the area of accelerator design has evolved. Through exposure, familiarity with the jargon can create the illusion of knowledge. It is the purpose of the primer to explain the fundamental principles and terminology and to bring substance to the jargon of accelerator design.

The primer is divided into four sections; Introduction, Fundamentals of Charged Particle Optics, Single Particle Optics, and Collective Particle Optics. In the Introduction, the purpose of the primer is explained and the beam optics of an NPB introduced. In the second section, Fundamentals of Charged Particle Optics, the concepts of phase space, nonlinear dynamics, linear maps, emittance, brightness, beam ellipse, machine ellipse, envelope equation, and a special applications section on the beam expansion telescope and the steering magnetic as used in an NPB device are presented. In the third section, Single Particle Optics, the differential equations used to calculate the motion of a charged particle in an arbitrary magnetic field are derived and the perturbative method of solving them is explained. The correspondence between the nonlinear terms of these equations and the geometric and chromatic aberrations of a magnetic optics system is discussed. Within this section, the matrix method of solving the linear optics of a drift space, a dipole, quadrupole, and combinations of them, is explained. The second and higher order contributions to quadrupole systems (doublets and triplets) are discussed. In the final section, Collective Particle Optics, the contribution of the Coulomb interaction among charged particles in a beam is described and some techniques for calculating the "space charge" effect in quadrupole systems and an achromatic bend are described.

The level of difficulty varies greatly throughout the primer. To some extent it reflects the level of mathematical sophistication required. For the reader with considerable technical experience some sections can be read very quickly. For those less experienced in mathematics and physics sections 3 and 4 will be challenging.

1.2 Introduction to Neutral Particle Beam Optical Systems

Before we begin our study of magnetic optics, an overview of beam transport systems for a NPB device will be given. Although many concepts have not yet been explained, this will serve as a useful reference.

A NPB device is used to produce a high current, high energy beam of neutral particles that are focused to a small spot on a distant target. The size of the spot may be as small as a few centimeters at a target distance of hundreds of kilometers. A generic NPB device is shown in Fig. 1. It consists of a sequence of components starting at the ion source, followed by the radio frequency quadrupole (RFQ), the buncher, the linear accelerating section, such as a drift tube linac (DTL), the matching section, the 180° achromatic bend, beam expansion telescope with momentum compactor, the steering magnet, the neutralizer and the beam sensing device. In this primer we will not describe the NPB system components preceeding the matching section. We will be concerned only with the beam optics components following acceleration. The beam optics of these components is so complicated that sophisticated computer codes are used in their design. These calculations and a full discussion of the design is outside the scope of this primer. We can only explain the physical concepts and mathematical techniques that are used to develop these computer codes.

Throughout the entire high energy beam transport (HEBT) system, re-occurring problems are faced by the designer.
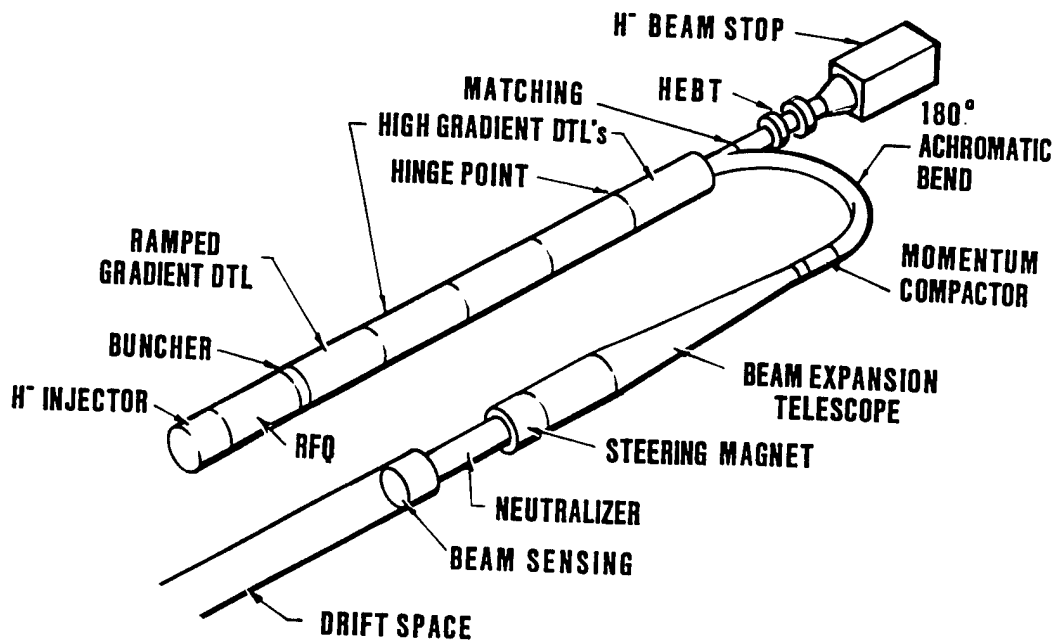
Figure 1. Generic Neutral Particle Beam Device

The first of these begins as the beam leaves the accelerating
section, where it starts to spread both transversely and
longitudinally unless confined by magnetic or electric forces.
This spreading is caused by the Coulomb repulsion of the charged
particles in the beam, the energy spread of the particles in the
beam, and the variation in the direction of the beam particles, the
divergence. Quadrupoles, magnets with two north and two south
poles, are used as lenses to confine the beam. The particles
exiting the accelerator portion of the NPB devices are bunched
longitudinally and are oscillating transversely at a frequency
defined by the r.f. fields of the accelerating structure. A
sequence of quadrupoles, focusing and defocusing, are used in the
section between the acceleration section and the 180° achromatic
bend, to match the short period of the accelerator to the long

4

period of the bend. The main concern of the designer of the matching section is how to maintain its ability to compensate for fluctuations in the beam current and energy without increasing the beams emittance. The concept of matching beams and beam emittance are discussed in detail in sections 2.4-8. As with all other magnetic optics devices, the matching section must be aligned with high precision and be capable of rapid re-adjustment to compensate for vibration and misalignment.

The 180° achromatic bend is a sequence of quadrupoles, used to focus and defocus the beam, and dipoles used to bend the beam. It is designed in periodic sections which consists of FODO cell, in which the total phase advance is a multiple of 360°. An achromatic bend is designed so that the first and second order aberrations are eliminated. This is discussed in detail in section 4.2. The use of sextupoles to correct chromatic aberrations is discussed in section 3.9. The designer must decide on the number and location of the quadrupoles and dipoles in the bend. This will determine the field strengths and the aperture of the magnets. As was the case with the matching section, the alignment of the magnets in the bend is critical. Also they must be adjustable so as to maintain an adequate acceptance as the beam current and energy varies. A major concern is the effect of nonlinear space charge. The contribution of the linear space charge has been calculated and some additional design constraints have been recognized by the designers. This is discussed in detail in section 4.3. It is suspected that the nonlinear space charge will significantly increase the emittance since it is known to mix the transverse and longitudinal emittance. To

understand the effect of space charge on emittance sections 2.4 through 2.9 should be read carefully. Another concern in the 180° bend is the effect of image charges, which are induced on the bend walls. Some calculations, made to estimate their effect, indicate that they are small.

After the beam exits the 180° bend, it enters the eyepiece of the beam expansion telescope. The eyepiece consists of a set of quadrupoles (typically three) which are used to focus the beam to produce an expansion of the beam beyond the focal point. The beam must be expanded so the divergence of the beam on exit from the objective lens of the telescope is very small. The objective of the telescope is a sequence of quadrupoles. Configuration of two, three and four quadrupoles have been investigated. Designing with quadrupoles is difficult because, when they are focusing in one transverse direction, they are defocusing in the orthogonal transverse direction. The selection and location of quadrupoles is a balancing act in the two transverse directions. The problems associated with quadrupole triplets are discussed in some detail in section 3 where the matrix representation for quadrupoles is used to calculate beam dynamics in composite systems. Analytic and numerical studies have been made of quadrupole doublets, triplets and quadruplets. The quadruplet has been found to be preferrable. Its main advantages are that the maximum transverse excursion is much less in the quadruplet than in the doublet. It is also more symmetric in the two transverse directions in the quadruplet.

The major concern in the telescope is geometric and chromatic aberrations. The geometric aberrations are caused by the nonlinearities in the magnetic fields of the quadrupoles.

6

They are produced by field inhomogeneities, misalignment, and fringe fields. The chromatic aberrations are a result of nonlinearities which depend on the dispersion and the spread in the energy of the beam particles. An extensive discussion of nonlinearities is contained in section 2.1 and the relationship between nonlinear fields and aberrations is discussed in sections 3.8 and 3.9. Designing systems which reduce or eliminate these nonlinear effects is difficult. It requires the calculation of the contributions of higher order terms in the beam dynamics equations. In some cases, sextupoles and octupoles can be used to make corrections. As usual, vibration and magnet misalignment can produce very significant effects in the telescope. The magnets of the objective lens are very large, more than a meter in diameters, and heavy. Maintaining alignment will be difficult. As in the bend, nonlinear space charge is very important in the telescope. The effect of space charge in quadrupole systems is discussed in section 4.2. There is a simple mathematical discussion of the beam expansion telescope in section 2.12.

To reduce the chromatic aberrations in both the telescope and the steering magnet (a dipole), a momentum compactor or r.f. deflector is used. A momentum compactor is an r.f. cavity which uses the separation of particles that occurs as the beam drifts. During a drift, the faster particles lead and the slower particles lag. The momentum compactor reduces the spread in the beam momentum by retarding the fast particles and accelerating the slow ones. The momentum compactor is located just after the eyepiece before the beam expands. Prior to reaching the compactor, the beam must have a long drift space so particle separation can take place. The r.f. fields

in the momentum compactor are timed so the lead particles experience a retarding force and the trailing particles an accelerating force. By using several cavities, harmonics of one another, it is possible to approximate a linear force. This is preferred because the beam has spread linearly during the drift. Since the accelerators operate at such high frequency, the momentum compactor is required to operate at this high frequency. It has not been demonstrated that a momentum compactor can be constructed capable of performing this function at these high frequencies. This will need to be demonstrated.

The steering magnet must have a bore as large as the objective quadrupoles of the telescope. It must be designed to minimize geometric and chromatic aberrations discussed earlier. It must be precisely aligned and it must be able to retarget rapidly using time varying magnetic fields. These fields produce special design problems. There is a simple discussion of the steering magnet in section 2.12.

Before concluding this discussion of the HEBT, it should be emphasized that one can work to reduce the emittance growth and the effects of geometric and chromatic aberrations, but they cannot be totally eliminated. The process of eliminating one produces or increases another one. For example, one may be able to reduce an aberration by increasing the length of the telescope but this will increase another aberration. For an example, the reader is referred to the telescope discussion in section 2.12. The only way these complicated systems can be optimized is with the use of computer codes. The codes must incorporate as much of the beam

dynamics as possible. In particular they must treat the problem
in three dimensions and include higher order nonlinearities and
nonlinear space charge. To obtain good system designs very good
computer codes are required.

All of these devices must be designed to maintain the small
transverse and longitudinal emittance produced in the accelerator
section. A small emittance is needed to produce a small beam
divergence, and a small beam divergence is needed to produce a
small spot. This relationship is explained in detail in the
discussion of emittance in section 2.3 and 2.12. To illustrate,
consider this simple example. To obtain a small spot (10 cm) on
target at a distance of 100 kilometers the angular spread α must
be equal to 10^{-6} radians (one microradian). This can be
demonstrated using elementary trigonometry. If the distance to
the target is d, the angular spread of the beam is α, and the spot
size is s, then

$$\tan \alpha = s/d \quad . \tag{1.1}$$

If s = 0.1 meters and d = 10^5 meters, and for small angles
$\tan \alpha \simeq \alpha$, so the divergence is

$$\alpha = 0.1 \text{ meters}/10^5 \text{ meters} = 10^{-6} \text{ radians.} \tag{1.2}$$

9

Fundamentals of Charged Particle Optics

2.1 Introduction

A charged particle beam consists of particles which can be
described by the physical properties of mass and electric charge.
Its dynamics can be described by specifying the locations, the
momenta and energy of the particles in the beam and the time. The
locations are specified by three spacial coordinates, the momenta
by the three components of momentum. These fundamental properties
determine how the particles interact with electromagnetic fields
and their resulting motion. A charged particle beam can contain a
large number of particles. For example, a beam with a current of
100 mA (milliamps) has a flow of 6.25×10^{17} particles/sec
(assuming that the particles have a charge of 1.6×10^{-19}
coulombs, the charge of a single electron). This large number of
particles is impossible to track even with the largest and fastest
computers. Fortunately to design a charged particle optical
system, this is not required.

Before beginning the discussion of single particle motion
some fundamental concepts are needed. There are many concepts from
classical electromagnetics, dynamics, and statistical mechanics
which are used to design beam optics systems that could be
included in this section. However, we can focus on only a few
important concepts: phase space, nonlinear dynamics, emittance,
beam ellipse, machine ellipse, acceptance, and beam envelope.

2.2 Phase Space and Nonlinear Motion

The concept of phase space is used to visualize the motion of
both a single particle and collections of particles such as those

in a particle beam. Since the motion of a particle is described by time evolution of its three orthogonal spacial coordinates x, y, z (usually thought of as the directions corresponding to left to right, down to up and in to out) shown in Fig. 2 and the
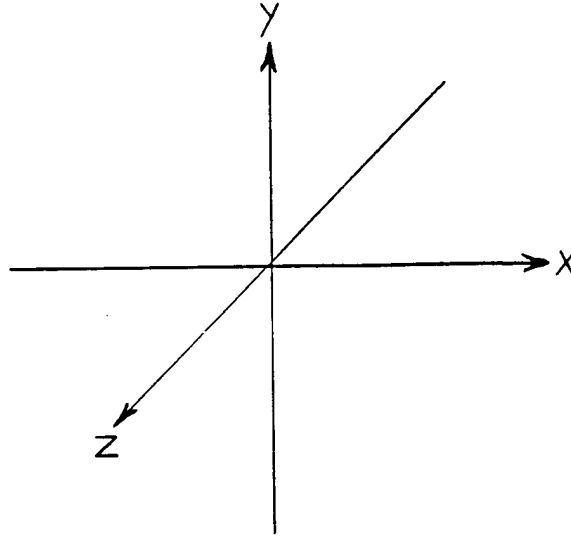
Figure 2.   An orthogonal three dimensional coordinate system (the arrows in the lines indicate the direction of increase in positive value of the variable)

corresponding momenta (as defined in classical mechanics as the product of the mass of the particle times its velocity). If a particle is moving parallel to the x-axis, then its momentum is the product of its mass, m, times the rate of change of x with time, its velocity, v_x. Thus

$$p_x = mv_x \tag{2.1}$$

The total momentum p is the vector sum of the momentum in the three directions

$$p = mv_x \hat{i} + mv_y \hat{j} + mv_z \hat{k} \tag{2.2}$$

where $\hat{i}$, $\hat{j}$ and $\hat{k}$ are the unit vectors which denote the direction in each of the axes. Since a single particle's motion is uniquely

11

defined by the three coordinates and three components of momentum,
the state of a particle is completely specified by a point in a
six dimensional space.

To simplify the discussion, we consider the one dimensional
problem by setting $y = z = v_y = v_z = 0$. Each point in a two
dimensional space is defined by a unique set of values for x and
p_x.
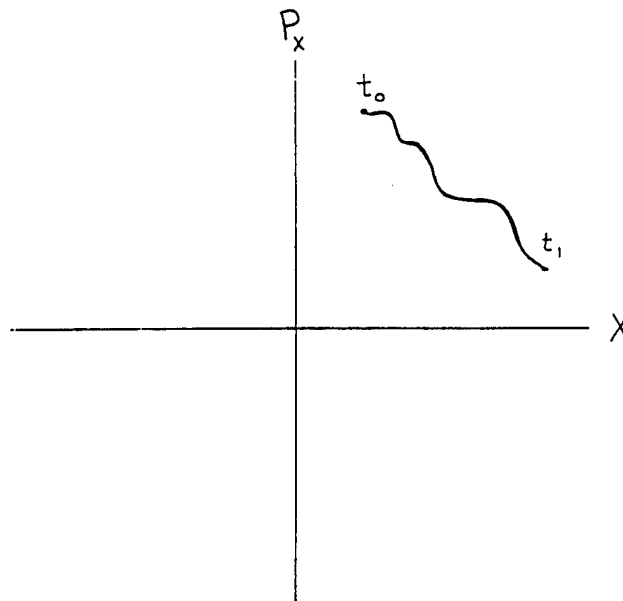
Figure 3.   Trajectory of a particle in the two dimensional
            phase space (x, p_x)

As time passes, the point in the x, p_x plane will change. The path
traced by the sequence of points when time goes from t_0 to t_1 is
called a trajectory in phase space and displays the history of the
particle's motion. For the full three coordinate and three momenta
problem, a six dimensional space is used, and the particle follows
a trajectory in this phase space. A phase space can be defined
using variables other than the position and momentum. The
selection of the variables depends on the problem to be solved.

12

The relationship between trajectories in phase space and the motion of a particle, can be shown by a particle executing simple harmonic motion in one spacial dimension. Its phase space is two dimensional (x, p_x). The force on this particle can be written as

$$F = - kx \qquad (2.3)$$

where F is the force, x is the displacement from the equilibrium point (that of zero force, $F = 0$). The position x and momentum p_x are related by Newton's Second Law of Motion

$$F_x = \dot{p}_x \ (= m\ddot{x}) \qquad (2.4)$$

where the dot over the p denotes the time rate of change of p (the first derivative of p with respect to time). By combining Eq.'s (2.3) and (2.4), we have the differential equation

$$\ddot{x} = - (k/m) \ x \qquad (2.5)$$

whose solution as a function of time is

$$x = a \sin (\omega t + \delta)$$
$$p_x = ma\omega \cos (\omega t + \delta) \qquad (2.6)$$
$$\dot{p}_x = -ma\omega^2 \sin (\omega t + \delta)$$

where a is the maximum displacement, ω is the frequency of the oscillation, and δ is the phase angle. Two initial conditions are needed to specify the particle's motion, the position and momentum at $t = 0$ denoted by x_0 and p_0. Thus

$$x(t = 0) = x_o = a \sin \delta$$

$$p_x(t = 0) = p_o = a \, m\omega \cos \delta \tag{2.7}$$

Thus, the phase and maximum amplitude are obtained from

$$\delta = \tan^{-1} (m\omega x_o/p_o) \text{ and } a = (x_o^2 + (p_o/m\omega)^2)^{1/2}$$

Using Eqs. (2.6) and (2.7) we see that $k = m\omega^2$ so that the frequency ω is

$$\omega = \sqrt{k/m} \tag{2.8}$$

This is a simple example of how the motion of a particle can be obtained using classical dynamics if the forces acting on the mass are known. For this harmonic oscillator, there is a constant of the motion, the total energy E

$$E = \frac{p_x^2}{2m} + \frac{1}{2} kx^2 . \tag{2.9}$$

Using Eq.'s (2.6), Eq. (2.9) can be written

$$E = \frac{ma^2\omega^2}{2} \cos^2 (\omega t + \delta) + \frac{a^2 m\omega^2}{2} \sin^2 (\omega t + \delta) \tag{2.10}$$

$$E = ma^2\omega^2/2 = \frac{1}{2} k a^2 \tag{2.11}$$

which is independent of time.

The phase space plot of the harmonic oscillator through one

14
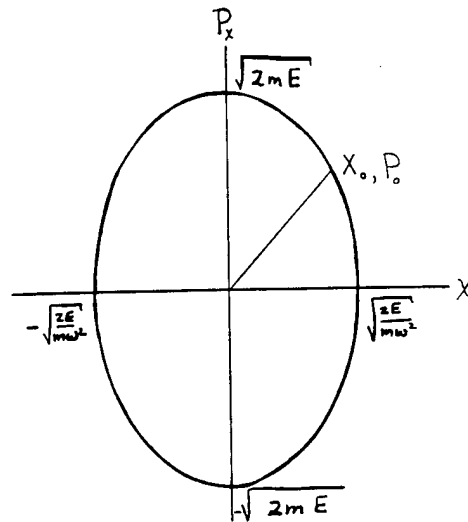
Figure 4. Phase space trajectory of a harmonic oscillator.

complete cycle is an ellipse as shown in Fig. 4. The maximum

values of x and p_x are determined by the energy and mass and the

frequency of the oscillation. Thus, we have shown that a periodic

oscillation in one dimension corresponds to a closed trajectory in

phase space. The particle will continue to follow the same

trajectory regardless of the original phase. This same motion

could be displayed graphically as a series of phase plots at

discrete times. For the harmonic oscillator the sequence is shown

in Figure 5.
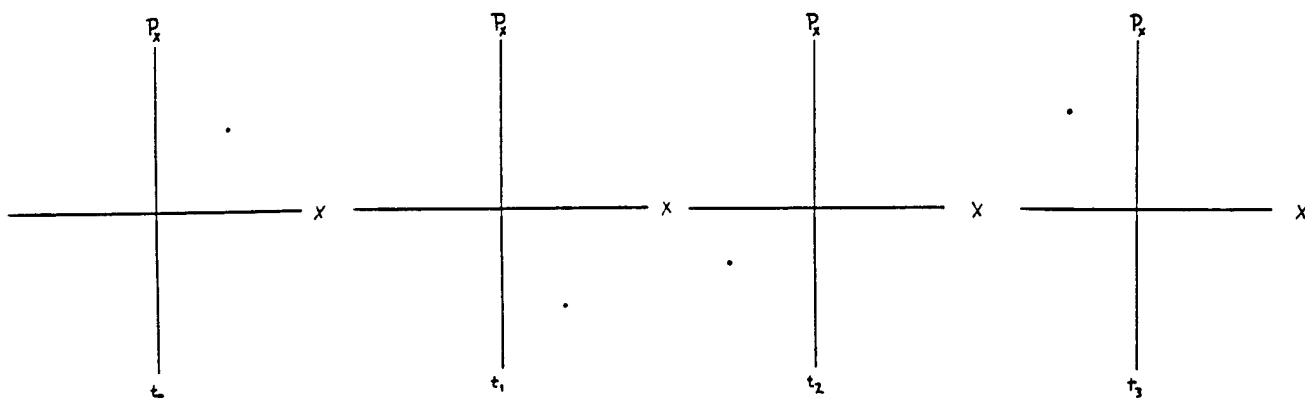
Figure 5. Series of phase space plots of a harmonic oscillator.

In this case, unless you have very small time steps compared to the period of oscillation $T = 2\pi/\omega$, it is very difficult to follow the trajectory. Also, if the trajectories of many particles are plotted in the same phase space, it is very difficult to follow them on the same plot.

A collection of like particles executing harmonic motion and having the same initial phase angle but slightly different energies, produce a series of phase space plots shown in Fig. 6.
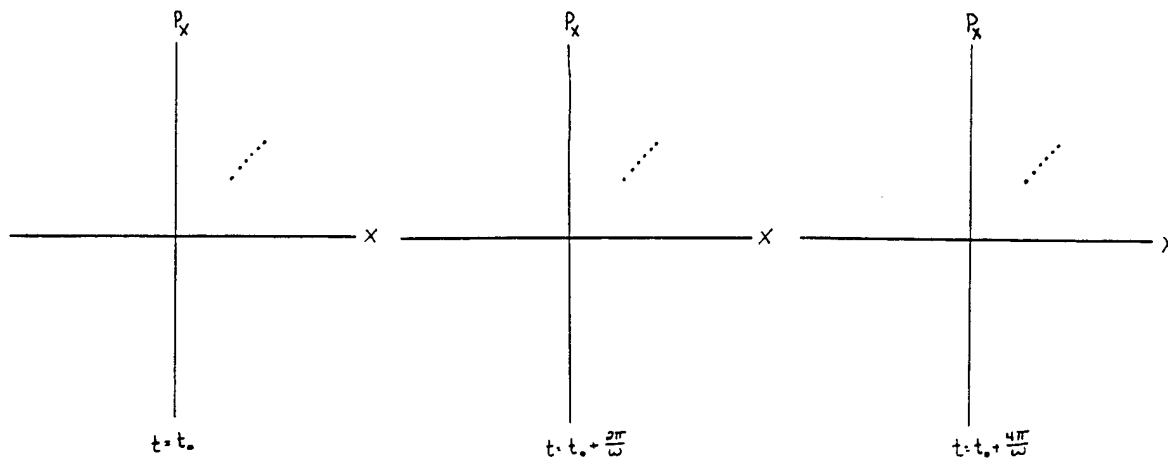
Figure 6. Phase space plots of particles with the same phase angle but with slightly different energies

Since the time to a complete one oscillation, the period, does not depend on the energy, see Eq. (2.8), particles initially localized will remain localized since they return to the same location in phase space after one period.

If nonlinear forces are added which involve powers of the displacement, a new force expression is obtained

$$F = -k_1 x + k_2 x^2 - k_3 x^3 \tag{2.12}$$

Observe that when k_2 and k_3 are zero, the linear case, the force for both positive and negative values of x are in the direction toward the equilibrium point at x = 0, and is said to be restoring. The quadratic term, with k_2 nonzero, cannot be restoring for both positive and negative displacements. In the case where k_1 and k_3 are zero, there is no equilibrium point and the motion is unbound for any initial displacement.

The energy for this anharmonic oscillator whose force is given in Eq. (2.12) is

$$E = \frac{p_x^2}{2m} + \frac{k_1 x^2}{2} - \frac{k_2 x^3}{3} + \frac{k_3 x^4}{4} \tag{2.13}$$

The kinetic energy (energy of motion) in Eq. (2.13) is $p_x^2/2m$, and the potential energy U is

$$U = k_1 x^2/2 - k_2 x^3/3 + k_3 x^4/4 \tag{2.14}$$

If we plot U versus x, we have the graph shown in Fig. 7, when $k_3 = 0$.

The motion of the anharmonic oscillator is bounded if the energy is less than the escape energy E_c, where

$$E_c = k_1^3/6k_2^2 \ , \tag{2.15}$$

since the particle will not have sufficient energy to overcome the potential barrier, the bump in Fig. 7. If the initial energy is greater than E_c, the motion will be unbounded. A plot of the potential energy with the cubic term added ($k_3 > 0$), is shown in Fig. 8.
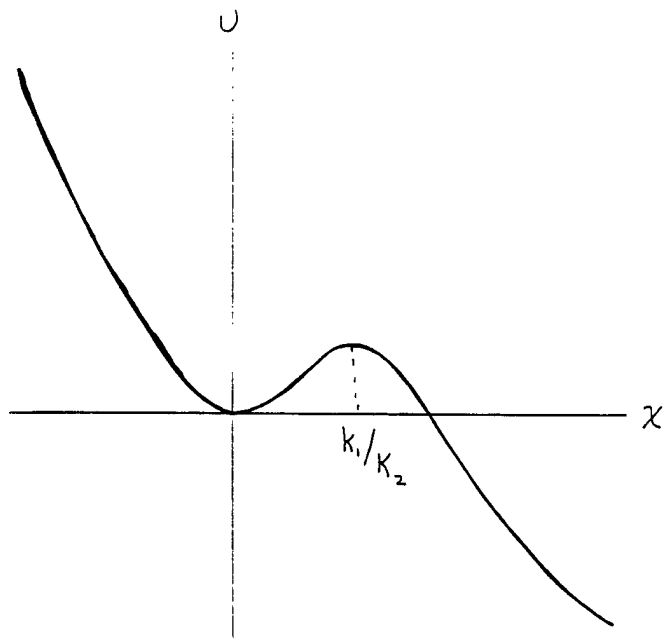
Figure 7. Plot of potential energy versus dispacement of
an anharmonic   oscillator with $k_3 = 0$
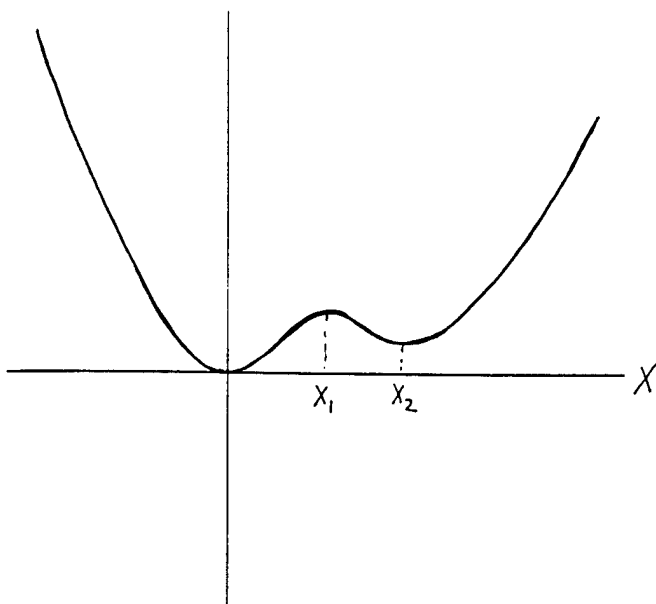
Figure 8. Plot of the potential energy versus displacement
of the anharmonic oscillator with $k_3 > 0$

In the case shown, the sign of k_3 is positive, the motion is bounded. The actual shape of the curve of Fig. 8 depends on the relative magnitudes of k_1, k_2, k_3. For some values there will be no equilibrium point at x_2 as shown in Fig. 8. For a potential as shown in Fig. 8, stable oscillations are possible about $x = 0$ and x_2.

Using Newton's Second Law, we obtain the second order differential equation in x,

$$m\ddot{x} = - k_1 x + k_2 x^2 - k_3 x^3 \qquad (2.16)$$

The solution to this equation can be written in terms of the Jacobi elliptic functions which are generalizations of the circular functions (sines and cosines). Unlike the linear case where the frequency ω is independent of energy, see Eq. (2.8), the frequency of oscillation for the anharmonic oscillator does depend on the energy. The phase space trajectories of an anharmonic oscillator ($k_3 = 0$) are shown in Figure 9.
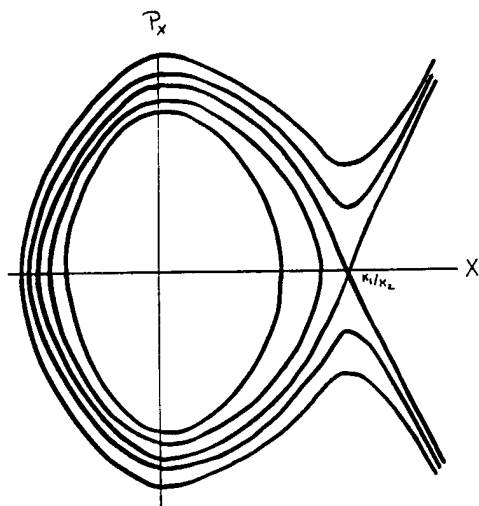
Figure 9. Phase space trajectory of an anharmonic oscillator with $k_2 > 0$, $k_3 = 0$

In Fig. 9, the trajectories for energies less than the escape energy, $k_1^3/6k_2^2$, are closed, the motion is bounded and periodic, but for energies greater than the escape energy the trajectories are unbounded. Note that the trajectories have larger excursion from the equilibrium point for positive values of x and smaller excursion for negative values of x.

Now that we understand the motion of a single oscillator or particle, we can investigate the many particle case. Imagine placing several particles, noninteracting, in the phase space of Fig. 9. If all of them have nearly the same energy, which is less than the escape energy, they will all follow periodic trajectories but with different periods. Thus the time for each to make one complete trip around the loop will differ. Recall that the period is a function of energy, so that particles will arrive at their starting point at different times. Therefore, a bunch of particles starting in the same region of phase space will become distributed (dispersed) about the phase space with the passage of time.

Before concluding this discussion of motion in phase space, we consider a few other ideas. Let us assume that the k_1, k_2, k_3 vary with time, not as a continuous function of time but change suddenly or jump and then remain constant between jumps. An example of such a case is shown in Figure 10. This produces a sequence of
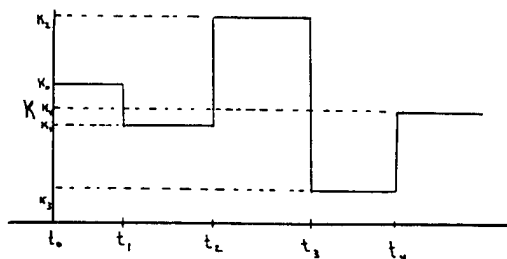
Figure 10. Plot of k versus time, t

phase space trajectories which change with each change in the
value of k. The trajectories appear as segments as illustrated in
Figure 11.
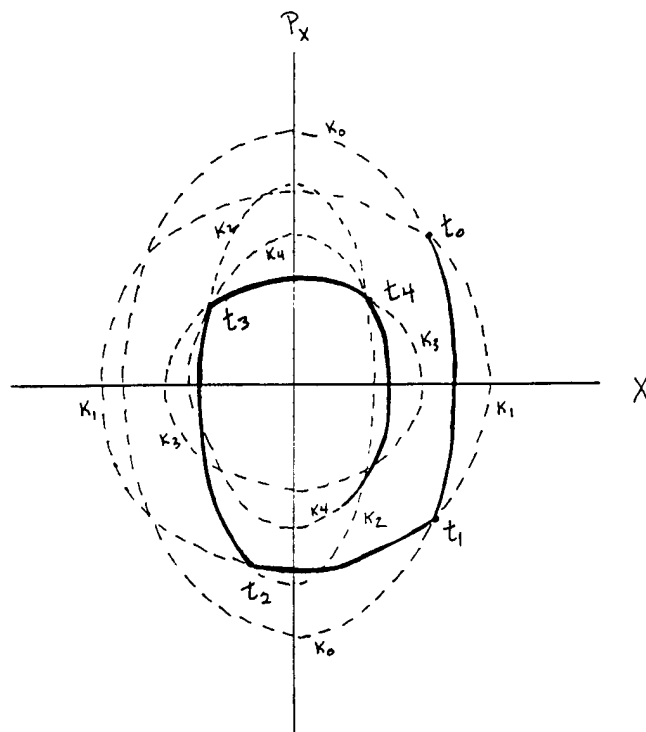
Figure 11. Trajectory in phase space for a sequence of
anharmonic oscillators

In the following section on single particle optics it will be
shown that the equations which describe the transverse motion of
the beam particles, (those perpendicular to the direction of beam
propagation), are those of the anharmonic oscillator but in more
than one dimension. It will be shown that as the beam travels
through the transport system, a sequence of optical elements, its
motion is described by a sequence of anharmonic (nonlinear)
oscillators with changing values of k. The anharmonic oscillator
equations are used because all continuous nonlinear forces can be
expressed as a power series whose lower order terms are assumed to
dominate. However, this is not true for space charge forces.

2.3 Linear Maps

Until now we have considered motion that can be described continuously in time. The equations which describe this motion are differential equations and the functions are sines and cosines or the elliptic functions. It is possible to calculate the transport of a particle through a beam optical system in the linear approximation by using linear maps. An example of a linear map is

$$X_1 = M_{11}X_0 + M_{12}P_0$$

$$\hspace{10cm} (2.17)$$

$$P_1 = M_{21}X_0 + M_{22}P_0$$

For the harmonic oscillator, which also applies to all linear cases, the map can be represented by a matrix, an array of elements in columns and rows. Matrix algebra, rules for multiplying matrices and vectors, is used to simplify these calculations. A vector y can be written as a column whose elements are the components of the vector. The position of a particle can be written as a vector whose components are the x, y and z values. The momentum can be written as a vector whose components are p_x, p_y, p_z. A vector of six components can be formed by combining the position and momentum vectors to obtain (x, p_x, y, p_y, z, p_z). As a column vector, labeled W, this vector can be written

$$W = \begin{pmatrix} x \\ p_x \\ y \\ p_y \\ z \\ p_z \end{pmatrix} \hspace{4cm} (2.18)$$

Thus the components of W can be written $w_1 = x$, $w_2 = p_x$, $w_3 = y$, $w_4 = p_y$, $w_5 = z$ and $w_6 = p_z$. The map denoted by M, can be written as a matrix with thirty-six elements

$$M = \begin{pmatrix} M_{11} & M_{12} & M_{13} & M_{14} & M_{15} & M_{16} \\ M_{21} & M_{22} & M_{23} & M_{24} & M_{25} & M_{26} \\ M_{31} & M_{32} & M_{33} & M_{34} & M_{35} & M_{36} \\ M_{41} & M_{42} & M_{43} & M_{44} & M_{45} & M_{46} \\ M_{51} & M_{52} & M_{53} & M_{54} & M_{55} & M_{56} \\ M_{61} & M_{62} & M_{63} & M_{64} & M_{65} & M_{66} \end{pmatrix} \tag{2.19}$$

To simplify the expression, we consider only the x, p_x case. Thus W has only two components. Let $W(0)$ be the vector whose values are the dynamical variables at time t_0 and $W(1)$ be their values at t_1. Thus $w(1)$ can be calculated using

$$W(1) = MW(0)$$

or

$$\begin{pmatrix} W_1(1) \\ W_2(1) \end{pmatrix} = \begin{pmatrix} M_{11} & M_{12} \\ M_{21} & M_{22} \end{pmatrix} \begin{pmatrix} W_1(0) \\ W_2(0) \end{pmatrix} \tag{2.20}$$

Matrix multiplication with the column vector gives the result

$$\begin{pmatrix} W_1(1) \\ W_2(1) \end{pmatrix} = \begin{pmatrix} M_{11} W_1(0) + M_{12} W_2(0) \\ M_{21} W_1(0) + M_{22} W_2(0) \end{pmatrix} \tag{2.21}$$

thus

$$W_i(1) = \sum_{j=1}^{2} M_{ij} W_j(0) \tag{2.22}$$

23

The sequence of linear maps can be written in matrix form as

$$
M_2 M_1 = \begin{pmatrix} M^{(2)}_{11} & M^{(2)}_{12} \\ M^{(2)}_{21} & M^{(2)}_{22} \end{pmatrix} \begin{pmatrix} M^{(1)}_{11} & M^{(1)}_{12} \\ M^{(1)}_{21} & M^{(1)}_{22} \end{pmatrix} \tag{2.23}
$$

$$
M_2 M_1 = \begin{pmatrix} M^{(2)}_{11} M^{(1)}_{11} + M^{(2)}_{12} M^{(1)}_{21} & M^{(2)}_{11} M^{(1)}_{12} + M^{(2)}_{12} M^{(1)}_{22} \\ M^{(2)}_{21} M^{(1)}_{11} + M^{(2)}_{22} M^{(1)}_{21} & M^{(2)}_{21} M^{(1)}_{12} + M^{(2)}_{22} M^{(1)}_{22} \end{pmatrix} \tag{2.24}
$$

The ij element of the matrix product is

$$
(M_2 M_1)_{ij} = \sum_{k=1}^{2} (M^{(2)}_{ik} M^{(1)}_{kj}) \tag{2.25}
$$

To illustrate how the matrix method is used, we calculate the matrix elements for the harmonic oscillator. From Eq's. (2.6) and (2.7), we have

$$
\begin{aligned}
x &= x_0 \cos\omega t + (p_0/m\omega) \sin\omega t \\
p_x &= p_0 \cos\omega t - m\omega x_0 \sin\omega t
\end{aligned} \tag{2.26}
$$

In matrix notation this can be written

$$
\begin{pmatrix} x \\ p_x \end{pmatrix} = \begin{pmatrix} \cos\omega t & 1/m\omega \, \sin\omega t \\ -m\omega \, \sin\omega t & \cos\omega t \end{pmatrix} \begin{pmatrix} x_0 \\ p_0 \end{pmatrix} \tag{2.27}
$$

Note for this case the matrix elements are continuous functions of time. It will be shown later in the single particle section that the elements do not need to be functions of time. For the case of a sequence of two oscillators with different k values, the matrix equation is

$$\begin{pmatrix} x(t_2) \\ p_x(t_2) \end{pmatrix} = \begin{pmatrix} \cos\omega_2(t_2-t_1) & 1/m\omega_2 \sin\omega_2(t_2-t_1) \\ -m\omega_2 \sin\omega_2(t_2-t_1) & \cos\omega_2(t_2-t_1) \end{pmatrix} X$$

(2.28)

$$\begin{pmatrix} \cos\omega_1 t_1 & 1/m\omega_1 \sin\omega_1 t_1 \\ -m\omega_1 \sin\omega_1 t_1 & \cos\omega_1 t_1 \end{pmatrix} \begin{pmatrix} x_0 \\ p_0 \end{pmatrix}$$

where

$$\omega_2 = \sqrt{\frac{k_2}{m}} \quad \text{and} \quad \omega_1 = \sqrt{\frac{k_1}{m}} \quad .$$

(2.29)

Thus by using matrices it is possible to track the particle through a sequence of elements. Note that the matrix elements do not depend on the values of x and p. This is not true for the nonlinear case. This matrix method makes the calculation of the piecewise linear case much easier. Figure 11 shows a sequence of trajectories that corresponded to the k values shown in Figure 10. There is a map which corresponds to each segment of the trajectories as shown in Fig. 11.

2.4 Emittance and Brightness

It has been widely recognized that emittance alone is insufficient to describe the effects of space charge and optical aberrations on a charged particle beam. They will be described in detail in sections 3 and 4. The description of a beam of charged particles is a complicated topic conceptionally. For an in-depth discussion, the reader is referred to an excellent article by C.

Lejeune and J. Aubert, titled, "Emittance and Brightness: Definitions and Measurements," Ref. 12. The topics presented in this subsection are a summary of their article. It should be consulted for more detail or if further clarification is needed.

To design and evaluate the performance of a beam transport system, the energy distribution of the beam (kinetic energy and energy spread), the total beam intensity, and the time structure is needed. There are two analytical methods used to study the dynamics of charged particle beams. One method is the "paraxial ray formalism" (described in section 3) which uses second order differential equations to calculate particle trajectories in real space. In the linear approximation (called the Gaussian optics approximation), the particles are assumed to travel along the optical axis and only the linear transverse variation of the electric and magnetic fields are included. The equations are similar to those of corpuscular optics (light as particles). Beams in a transport system are not perfectly linear and nondispersive. They have a thermal velocity spread and are influenced by nonlinear forces which produce geometric and chromatic aberrations, and by space charge and element misalignment effects. The concepts of "emittance" and "brightness" have been added to the paraxial formalism in an attempt to solve these problems. As beam transport systems with higher currents and energies were being designed, the "Hamiltonian formalism" was adopted. An example of this method is the Lie algebraic method developed by A. Dragt. It is used to calculate trajectories of

26

points in phase space, as was described earlier in this section, and to study the evolution of the distribution of points defined by a density distribution function. Liouville's theorem, which for Hamiltonian systems states that the density in phase space is invariant along the trajectory of a given point, is used to express the emittance and brightness in terms of invariants (unchanging quantities). This will be explained in more detail later.

2.5 Hamilton Mechanics

For those familiar with classical mechanics the following brief description of the Hamiltonian formalism should be sufficient to understand the concepts of emittance and acceptance described later. For those not familiar with classical mechanics a standard text on the subject may need to be consulted.

The Newtonian equations of motion are identical to the Euler-Lagrange equations which use the Lagragian, a function of a set of generalized coordinates (positions) and their time derivatives $\dot{q}_i = dq_i/dt$ (velocities). A dynamical system which has k degrees of freedom can be described by 2k dynamical variables and time. The motion of a particle in a three dimensional space, three degrees of freedom, is described by six dynamical variables. The conjugate momentum in terms of the Lagrangian, $L(q_i, \dot{q}_i, t)$, is

$$p_i = \frac{\partial L}{\partial \dot{q}_i} \, . \tag{2.30}$$

A new function, the Hamiltonian $H(p_i, q_i, t)$ can be written in

27

terms of the Lagrangian as

$$H(p_i, q_i, t) = \sum_{i=1}^{k} p_i q_i - L \qquad (2.31)$$

The equations of motion, which consist of a set of 2k first order differential equations, can now be written as

$$\dot{q}_i = dq_i/dt = \partial H/\partial p_i$$
$$\dot{p}_i = dp_i/dt = -\partial H/\partial q_i \qquad (2.32)$$

For each degree of freedom, there is a pair of equations. A dynamical system is said to be Hamiltonian if there exits a function H which satisfies these equations of motion.

Starting with the time derivative of the Hamiltonian

$$\frac{dH}{dt} = \sum_{i=1}^{k} \left(\frac{\partial H}{\partial q}\frac{dq_i}{dt} + \frac{\partial H}{\partial p_i}\frac{dp_i}{dt}\right) + \frac{\partial H}{\partial t} \quad .$$

and using Eqs. (2.31) it can easily be shown that

$$\frac{dH}{dt} = \frac{\partial H}{\partial t} \quad . \qquad (2.33)$$

Thus the Hamiltonian is a constant of the motion, time independent, if it is not an explicit function of time. The Hamiltonian is identified as the total energy of a system if it can be written as a sum of the total kinetic energy and a velocity independent potential energy. For the particular case of electromagnetic forces which has velocity dependent forces, the Hamiltonian can still be identified with the total energy since the canonical momenta incorporate the velocity dependent vector potential.

28

2.6 Advanced Concepts in Phase Space, Liouville's Theorem and Brightness.

The motion of a dynamical system with k degrees of freedom can be represented by the position of a point with coordinates $(q_1, q_k, p_1, \ldots p_k)$ in a 2k dimensional space, "phase space". For a gas of N particles, each with three degrees of freedom, the system at time t would be represented by a set of points in 6N-dimensional phase space, "Γ_6 space". Associated with each set of points in Γ_{6N} is a real density in phase space described by f_{6N}, the density distribution in phase space. If the N identical particles are noninteracting, the Hamiltonian of each particle depends on only six coordinates and the motion is described by six equations. In this case the motion will be described by a trajectory in the six dimensional space Γ_6. The state of the whole system at an instant of time is described by a set of points in Γ_6, the real density in phase space. The distribution function of density $f_6(\vec{p}, \vec{q}, t)$ describes this density. The number of points near the point $\vec{p}, \vec{q}$ at time t is defined as

$$d^6N = f_6(p,q,t) \, d\mathcal{V}_6 \,. \tag{2.34}$$

If the motion associated with each degree of freedom is independent of the other two, the Hamiltonian can be separated into a sum

$$H(\vec{p}, \vec{q}, t) = H_1(p_1, q_1, t) + H_2(p_2, q_2, t) + H_3(p_3, q_3, t). \tag{2.35}$$

where the equations of motion for each are

$$\dot{p}_i = -\partial H_i / \partial q_i$$
$$\qquad\qquad i = 1, 2, 3 \tag{2.36}$$
$$\dot{q}_i = \partial H_i / \partial p_i$$

In this case, the motion of a particle can be represented by a

trajectory in each of three two-dimensional phase planes Γ_2 associated with each degree of freedom. Some properties of trajectories in phase space can be obtained using the Hamiltonian formalism, without a detailed knowledge of the individual trajectories. They can be summarized as follows:

1) The trajectories in phase space depend uniquely on the initial values (p_0, q_0) and the time. Thus trajectories starting at different points at the same time nowhere intersect. When the Hamiltonian is time independent, the trajectories in Γ_2 are independent of time and cannot intersect. For example, the trajectories for the harmonic oscillator are concentric ellipses. Oscillatory systems with finite periods have closed trajectories.

2) A boundary in the phase plane, c, that encloses a group of particles, at time t, will transform into a boundary c_2 at time t_2 enclosing the same group of particles.

3) Phase space domains bounded by straight lines or by ellipses are convenient to use for linear sytems of forces. In this case there exists a linear transformation which maps the initial coordinates into their final values. For linear transformations, straight lines map to straight lines and ellipses to ellipses. The area of the ellipse is conserved in linear systems, thus the emittance is conserved. This is used later in the discussion of the beam ellipse.

We are now ready to describe Liouville's theorem involving the density function f in phase space. It states that for a Hamiltonian system, the density of particles in phase space is invariant along the trajectory of a given point. This is based on the fact that

the total time derivative of the density distribution function is zero. As a result of Liouville's theorem, the shape of the domain boundary in phase space may change but the volume enclosed remains constant.

For a system of charged particles with external electric and magnetic fields to be Hamiltonian, it must satisfy several condtions. Wave mechanics is not needed to describe the system's behavior. There is no electromagnetic radiation. There are no close range interactions, such as collisions and no long range velocity dependent interactions such as those caused by collective space charge fields.

Liouville's theorem applies to f_{6N} for a system of N nonidentical particles each with three degrees of freedom in a 6N dimensional phase space Γ_{6N}. If all the particles are identical, it applies to f_6 in the Γ_6 phase space. If only two of the degrees of freedom are coupled, then it applies to f_4 in a Γ_4. If all the degrees of freedom are uncoupled then it applies to f_2 for each of three Γ_2 spaces. The $f_2(p_1, q_1)$ is defined as a projection of the Γ_6 onto a Γ_2 space, where

$$f_2(p_1, q_1) = \int\int\int\int f_6(p_1, q_1, p_2, q_2, p_3, q_3) dp_2 dq_2 dp_3 dq_3 \qquad (2.37)$$

and

$$N = \int\int f_2(p_1, q_1) dp_1 dq_1 \qquad (2.38)$$

The area in the q_1, p_1 space is

$$A = \int\int dp_1 dq_1 \qquad . \qquad (2.39)$$

This should not be confused with the density distribution function

$$d_2(p_1,q_1) \sim f_6(p_1,q_1,0,0,0,0) \tag{2.40}$$

which is a section of the Γ_6 phase space.

When interparticle coulomb forces are present, the conditions of Liouville's theorem are not satisfied. It has been proposed by Lichtenberg, ref. [13], that when there are very small correlations between particles, Liouville's theorem holds approximately in the Γ_6 phase space. This small correlation condition applies to situations where the number of particles in the Debye sphere surrounding any particle is large, thus when

$$\lambda_D \gg n^{-1/3} \approx \text{(spacing between particles)} \tag{2.41}$$

where n is the density of charged particles in real space and λ_D is the Debye length, the ratio of the thermal velocity, $(kT/M)^{1/2}$, to the plasma frequency $\omega_p = (q^2 n/M\varepsilon_o)^{1/2}$, where q and M are the particle charge and mass. In this case, the smoothed out potential, due to all the particles, can be calculated from the density distribution in real space and its contribution included in the Hamiltonian system of forces. An example of the procedure is discussed in section 4 on space charge effects.

We consider a beam consisting of identical, nonradiating, noninteracting particles each having their velocity component in the "direction of propagation" much larger than those of the transverse direction. In this case the motion of the particles in the beam can be represented by trajectories in Γ_6. In general, the axial and transverse motions are coupled and therefore they occupy a six-dimensional hypervolume in Γ_6 to which Liouville's theorem applies. The time evolution of the beam is described by the time

evolution of the distribution function $f_6(x,y,z,p_x,p_y,p_z;t)$.
The density distribution can be written with respect to the
design trajectory defined by z_q and its design momentum p_{oz}

$$f_6(x,y,\Delta z,p_x,p_y,\Delta p_z;z_q)$$

where $\Delta z = z - z_q$ and $\Delta p_z = p_z - p_{oz}$. This description is explained
in more detail in section 3. If z, the propagation coordinate, is
taken as the independent variable in place of time, the density
distribution relative to the reference particle can be written

$$f_6(x,p_x,y,p_y,\Delta t,-\Delta H;z) \ .$$

The Δt and ΔH correspond to the phase shift and energy difference.
If the transverse and axial motions are uncoupled, then the Γ_6
separates into a Γ_4 transverse space (x,p_x,y,p_y) and a Γ_2 axial
phase space $(\Delta z,\Delta p_z)$ or $(\Delta t,\Delta H)$.

Experimental results for the transverse motions are usually
expressed in the two planes x,x' and y,y' where x' and y' are the
gradients of the trajectories in the x-z and y-z planes. Thus

$$
\begin{aligned}
x' &= dx/dz \\
y' &= dy/dz
\end{aligned}
\tag{2.42}
$$

In the paraxial approximation $x' = \tan \alpha_x \approx \alpha_x$ and $y' \approx \alpha_y$. Thus
x' and y' are the direct measure of the angle between the particle
trajectory and the optical axis. These spaces (x,x') and (y,y')
are referred to as trace spaces. They are not phase spaces since
x' is not the conjugate momentum of x and y' is not the conjugate

momentum for y, and Liouville's theorem does not apply in these spaces. The relationships between the momentum p_x and x' is

$$p_x = m_o c \beta \gamma x' + qA_x \qquad (2.43)$$

where β and γ are the relativistic parameters for the axial motion,

$$\beta = v_z/c \text{ and } \gamma = 1/(1 - \beta^2)^{1/2} \qquad (2.44)$$

and A_x is the x component of the magnetic vector potential, (B=v x A). In the case where ($A_x = A_y = 0$), the volumes in phase and trace space are related by the expressions

$$\mathcal{V}_4 = (M_o c \beta \gamma)^2 V_4$$
$$f_4(x, p_x, y, p_y) = \rho_4(x, x', y, y')/(m_o c \beta \gamma)^2 \qquad (2.45)$$

where $\mathcal{V}_4$ is a volume in Γ_4 and V_4 is the volume in trace space.

The hyperemittance, ε_4, is related to the hypervolume V_4 enclosing all particles in the T_4 trace space:

$$\varepsilon_4 = V_4/\pi^2 \qquad (\pi^2 \text{rad}^2 \text{m}^2) . \qquad (2.46)$$

The brightness, B, is the average value of the density in trace space:

$$B = \overline{\rho}_4 = I/V_4 = I/\pi^2 \varepsilon_4 \quad (\text{A rad}^{-2}\text{m}^{-2}) . \qquad (2.47)$$

The brightness is conserved only when the force fields are Hamiltonian, no particles are created or lost, the axial and transverse motions are uncoupled, the axial velocity is constant over any cross section and along the optical axis and the magnetic field is entirely transverse ($A_x = A_y = 0$).

34

The normalized hyperemittance is the hypervolume in transverse phase space

$$\varepsilon_{4n} = \beta^2\gamma^2 V_4/\pi^2 = \beta^2\gamma^2\varepsilon_4 . \qquad (2.48)$$

The normalized brightness is

$$B_n = Im_o^2 c^2/\mathcal{V}_4 = B/\beta^2\gamma^2 . \qquad (2.49)$$

or

$$B_n = I/\pi^2\varepsilon_{4n} .$$

The density distribution functions are determined experimentally in the trace planes T_2. The emittance is defined by

$$\varepsilon^x = A_2^x/\pi \equiv \frac{1}{\pi}\int\int dx \cdot dx' \qquad (rad - m) . \qquad (2.50)$$

This definition of emittance is used for projections of distribution as described earlier. For the emittance in x and y directions to be invariant, the motions in the transverse directions must be uncoupled. The normalized emittance ε_n is defined by

$$\varepsilon_n^x = \mathcal{A}_2^x/\pi m_o c = p_z A_2^x/\pi m_o c \qquad (\pi \text{ rad-m}) . \qquad (2.51)$$

where $\mathcal{A}_2^x$ is the area in phase space, A_2^x is the area in trace space.

Optical elements in general produce magnetic fields that couple the transverse components of the beam. However, in an infinite magnetic quadrupole with hyperbolic pole pieces $(A_x = A_y = 0)$ the forces are linear and the x and y motions are uncoupled.

35

2.7 Acceptance

A beam transport system must be designed to guide a given beam of known current and emittance while reducing particle loss and the deterioration of the optical properties of the beam. The acceptance domain is the region of phase space in which the motion of all particles injected at the entrance will be transmitted without loss. The acceptance domain is equivalent to the maximum hyperemittance domain that a beam may occupy if it passes through the system without loss. For uncoupled transverse components the acceptance area in T_2

$$Y^X = A_2{}^X/\pi \tag{2.52}$$

and normalized acceptance

$$Y_n{}^X = \beta\gamma A_2{}^X/\pi \ . \tag{2.53}$$

When the emittance curve for each optical element can be brought into coincidence with a curve along which the Hamiltonian is constant for that element, recall the curve of constant energy for the harmonic oscillator, the emittance domain is unaltered during transport through the element. When this condition exists the beam is said to be matched to the optical element. A "matching section" is an optical element which performs this function.

When the forces are nonlinear, the angular velocities of rotation of the points in phase space vary with the radial distance. (This was discussed earlier for the anharmonic oscillator.) In this case the emittance diagram is deformed and filamentation occurs. For some cases it is believed that the

process of filamentation can be reversed which would correspond to the reversal of the nonlinear processes that created it, an unwinding.

The distribution of particles in a beam is not uniform. Most experimental beams have halos, that correspond to a tail in the distribution. As much as half the area occupied by a beam may contain only ten percent of the particles. To describe the beam, intensity-emittance characteristic curves are used. Equidensity contours are drawn on the emittance diagram. The fractional intensity that flows inside an equidensity contour (Σ) is plotted as a function of the enclosed emittance

$$I = \int \int_{\Sigma} \rho_2(x,x')dxdx'$$

$$\epsilon = \frac{1}{\pi} \int_{\Sigma} x'dx' \tag{2.54}$$

I_T and ϵ_T are the total intensity and total emittance of the beam. A "perfect beam" is one for which the projections in each of the planes (x,y), (x,x'), (y,y') and (y',x') of the trace space have a uniform density in elliptical boundaries. In Fig. 12 (a), the curve marked I is that of a "perfect beam", the curve II is for one with a uniform density in T_4, and curve III is for the Guassian distribution in T_4 or T_2. The curve for real beams are characterized by two emittances ϵ_{90} and ϵ_c. The ϵ_{90} encloses 90% of the total intensity of the beam and ϵ_c is defined as the value of the emittance at which the line tangent to the emittance curve at the orgin has a value I_t, the total current, as shown in Fig. 12(b). For a Gaussian beam, 63% of the total intensity

37

correspondes to ε_C and 86.5% to $2\varepsilon_C$. These correspond to $\sqrt{2}$ and 2 times the standard deviation of the Gaussian function.
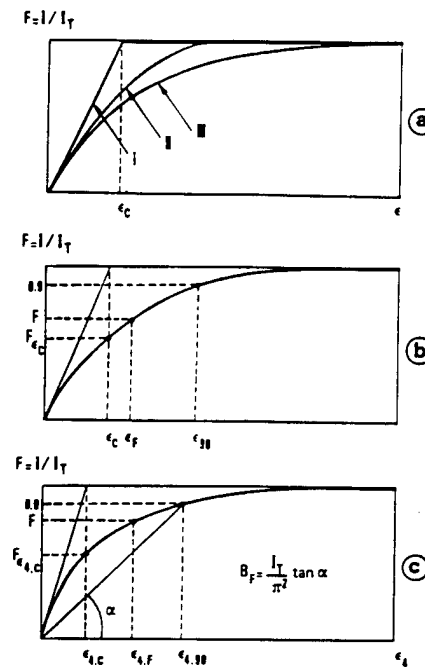
(a) "Intensity–emittance characteristics" for various hyperellipsoidal distributions: (I) Kapchinsky–Vladimirsky distribution of a "perfect beam"; (II) uniform density in T_4 four-dimensional trace space; (III) Gaussian distribution. (b) The meaningful parameters of an "intensity–emittance curve": ε_{90}, enclosing 90% of the total beam intensity, and ε_c, the "emittance constant" with its appropriate percentage of I_T, $F_{(\varepsilon_c)}$; for a Gaussian distribution, this is 63%. (c) The meaningful parameters of an "intensity-hyperemittance curve": $\varepsilon_{4,90}$ and ε_{4c}, the "hyperemittance constant," with its appropriate percentage of I_T, $F_{(\varepsilon_{4c})}$. ε_F and $\varepsilon_{4,F}$ are the emittance and hyperemittance enclosing the factor F of the total beam intensity.

Figure 12.   (Figure from Ref. [12])

2.8   RMS – Emittance

The concept of the root-mean-square (rms) emittance was introduced by Chasman et al (1969) in an attempt to relate the equivalent "perfect beam" to any real beam. For a real beam the projection on T_2 trace space is the density $\rho_2(x,x')$. The second moments are $\overline{x^2}$, $\overline{x'^2}$ and $\overline{xx'}$ which are related to the beam width, velocity spread and beam divergence. The equivalent perfect beam is defined as the perfect beam having the same intensity and the same second moments of the trace plane projected distribution,

38

$$x^2 = \frac{\int\int x^2 \rho_2(x,x')dxdx'}{\int\int \rho_2(x,x')dxdx'} \qquad (2.55)$$

For the "perfect beam", a uniformly filled ellipse, in which the half-width is x_{max} and the half-angular velocity spread is x'_{max}, see Fig. [15], it can be shown that

$$x_{max} = 2(\overline{x^2})^{1/2}$$
$$\qquad (2.56)$$
$$x'_{max} = 2(\overline{x'^2})^{1/2}$$

The emittance ε for an arbitrarily oriented ellipse is

$$\varepsilon = 4(\overline{x^2}\ \overline{x'^2} - (\overline{xx'})^2)^{1/2}$$

Using emitance expression for an "equivalent perfect beam", the emittance of a real continuous beam can be defined in terms of its second moments as

$$\overline{\varepsilon} = 4(\overline{x^2}\ \overline{x'^2} - (\overline{xx'})^2)^{1/2} \qquad (2.57)$$

and referred to as the rms emittance, see Ref. [14].

For a Gaussian hyperellipsoid distribution, 86% of the total beam intensity will flow within an ellipse of area $\overline{\varepsilon}$. For linear focusing systems, the rms emittance will be an invariant of the motion. In general the emittance in a Hamiltonian system is invariant, but the rms emittance $\overline{\varepsilon}$ is not. In linear systems the rms emittance is conserved by the linear transformations and not by Liouville's theorem.

2.9 Beam Ellipse

Since the number of particles in a beam is large, it is impossible to follow the trajectories through all the optical

elements. For the linear case it is easier to use a closed curve or surface in phase space that encloses all the particles or some fraction of them. Particles contained within the boundary initially will remain within the boundary in the linear case. An ellipse is usually selected for the curve which is centered on the origin having the general equation

$$ax^2 + 2bxx' + cx'^2 = 1 \ . \tag{2.58}$$

This can be written in matrix form

$$m = (x \ x') \begin{pmatrix} a & b \\ b & c \end{pmatrix} \begin{pmatrix} x \\ x' \end{pmatrix} \tag{2.59}$$

In matrix notation, Eq. (2.58) can be written

$$x^t B x = 1 \ . \tag{2.60}$$

We denote the inverse of the matrix B

$$\sigma = B^{-1} = \begin{pmatrix} \sigma_{11} & \sigma_{12} \\ \sigma_{21} & \sigma_{22} \end{pmatrix} \tag{2.61}$$

The inverse of a matrix is the matrix such that

$$B^{-1}B = I \tag{2.62}$$

where I is the identity matrix

$$I = \begin{pmatrix} 1 & 0 \\ 0 & 1 \end{pmatrix} \ . \tag{2.63}$$

The intercepts of the ellipse with the axis are shown in terms of the components of σ in Fig. 13.
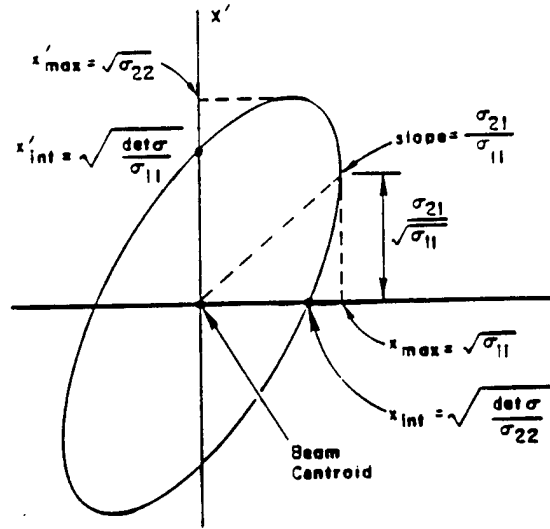
Figure 13.   A beam ellipse based on the σ matrix   The maximum extent of the ellipse and its orientation are shown as a function of the matrix elements.   (Figure from Ref. [2])

The area of the beam ellipse is $\pi\epsilon$ and the emittance $\epsilon = (\det B)^{-1}$ = det σ.   The determinant of a 2 x 2 matrix as in Eq. (2.58) is

$$\det B = ac - b^2 \qquad \text{and}$$
$$\det \sigma = \sigma_{11}\sigma_{22} - \sigma_{12}\sigma_{21} \qquad (2.64)$$

In the linear approximation, along the transport line the shape of the beam ellipse changes but its volume in phase space remains constant.

2.10 Machine Ellipse

Besides the beam ellipse, there is another useful ellipse, the machine ellipse. It will be described for closed machines, those in which the beam travels in a loop, i.e. the circular machines and storage rings. In these machines the particles make transverse oscillation similiar to that of the harmonic oscillator but the coupling parameter varies with time or

41

correspondingly with the passage around the ring, and are periodic functions since the machine is a closed loop. The general solution to the linear equations can be written

$$x(s) = \sqrt{\epsilon\beta(s)} \cos (\Psi(s)+\phi) \tag{2.65}$$

where s, the distance along the propagation direction, has replaced the time, t, and $\beta(s)$ and $\Psi(s)$ are periodic functions and ϵ and ϕ are arbitrary constants. The equation

$$\gamma(s)x^2 + 2\alpha(s)xx' + \beta(s)x'^2 = \epsilon . \tag{2.66}$$

where $x' = dx/ds, \alpha(s) \equiv - \beta'(s)/2$ and $\gamma(s) \equiv (1 + \alpha(s)^2)/\beta(s)$ can be obtained by eliminating the sines and cosines from the expression for x(s) and x'(s). The particle starting on the ellipse defined by Eq. (2.63) will return to a point on the ellipse after each cycle of the machine. Figure 14 shows the ellipse with the expressions for the maximum value for x and x' and the intercepts of each axis as functions of β, α, and γ.
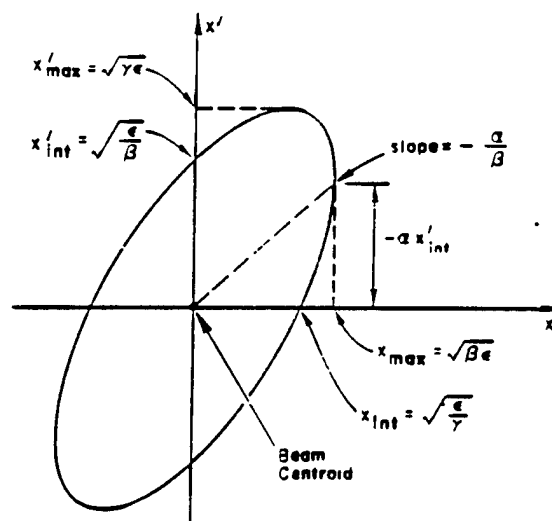
Figure 14. An ellipse based on the machine parameters β, α, γ, illustrating single-particle motion in a closed machine The area of the ellipse is $A = \pi\epsilon$. (Figure from Ref. [2])

42

The intercepts can easily be obtained by setting x and x' to zero in Eq. (2.63). The area of the ellipse is $\pi\varepsilon = \pi x_{max} x'_{inter} = \pi x_{inter} x'_{max}$.

The reader must be careful not to confuse the beam ellipse with the machine ellipse. When the beam ellipse and the machine ellipse are concentric and similar, the beam and machine are said to be matched; the particles in the phase space can be accommodated by the machine.

2.11 Envelope Equations

Instead of using the beam ellipse description above, it is possible to calculate the "envelope" or "envelope function" in place of the α and β of Eq. (2.66). The maximum amplitude of the ellipse and its derivative are related to α and β by the expressions

$$a = \sqrt{\varepsilon\beta}$$
$$a' = \alpha\sqrt{\varepsilon/\beta}$$

$$(2.67)$$

The beam ellipse Eq. (2.64), can be written

$$A^2x^2 - 2aa'xx' + a^2x'^2 = \varepsilon^2 \tag{2.68}$$

where A is the maximum angular deviation in the beam and $A = (\varepsilon^2/a^2 + a'^2)^{1/2}$. If Eq. (2.67) is differentiated with respect to s, we have

$$a''x - ax'' - \frac{\varepsilon^2}{a^3} = 0 \tag{2.69}$$

43
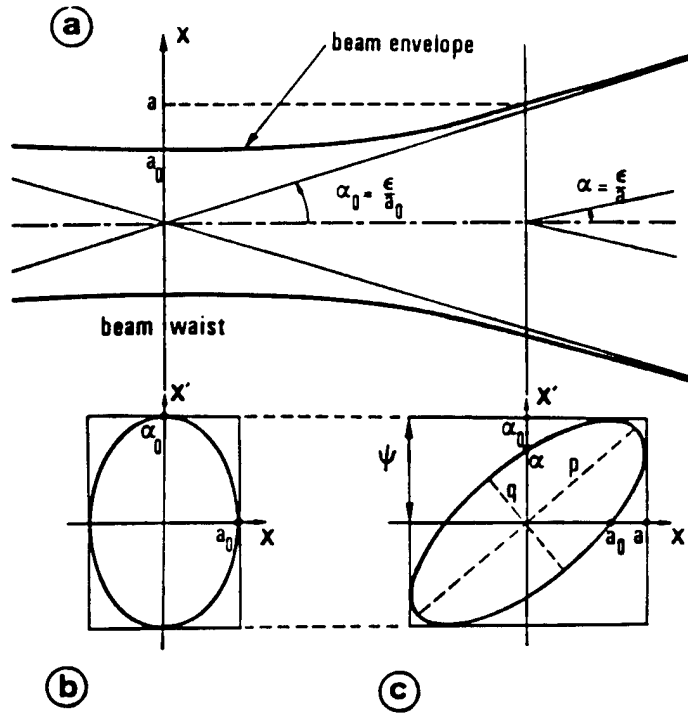
Emittance ellipse of a normal beam in terms of beam envelope. (a) Beam envelope in a drift space under the actions of emittance only: $\epsilon = a_0\alpha_0 = a\alpha$. (b) Upright emittance ellipse at the beam waist. (c) Oblique emittance ellipse downstream from the beam waist (diverging beam): $\epsilon = a\alpha = pq$. a is the beam half-width and ψ the semiangular spread.

Figure 15. (Figure from Ref. [3])

By replacing x" with the $\mp$ kx, the linear approximation to x",
we obtain the differential equation for a, the envelope equation,

$$a'' \pm ka - \epsilon^2/a^3 = 0 \qquad\qquad (2.70)$$

This differs from the trajectory equation (see Eq. (2.5)) by
the factor $-\epsilon^2/a^3$. This factor prevents the envelope, a, from
becoming negative.

2.12 The Beam Expanding Telescope and Steering Magnet

Before starting the next section on single particle optics we illustrate how the concept of emittance can be used to analyze the beam expanding telescope as shown in Fig. 16. The source of the following analysis was John Farrell, see Ref. [15].
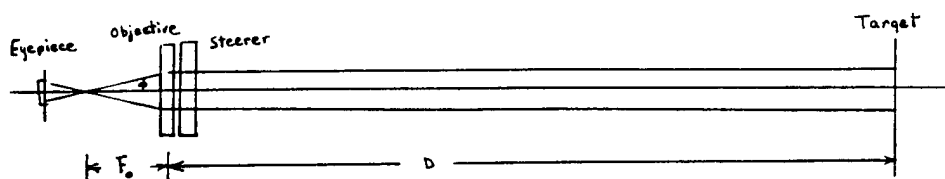
Figure 16. Beam Expanding Telescope with Steering Magnet.

We consider a charged particle beam with an rms divergence, x'_{max}, and a radius at the objective lens, x_{max}. The transverse laboratory emittance $\overline{\varepsilon}_{rms}$ is

$$\overline{\varepsilon}_{rms} = x_{max} x'_{max} \tag{2.71}$$

The normalized emittance $\overline{\varepsilon}_n$ is related to $\overline{\varepsilon}_{rms}$ by the expression

$$\overline{\varepsilon}_n = \beta\gamma\overline{\varepsilon}_{rms} \tag{2.72}$$

45

where

$$\beta = \frac{v}{c} = \left[1 - \frac{E_0^2}{E_t^2} \right]^{1/2} \quad , \tag{2.73}$$

$$\gamma = (1 - \beta^2)^{-1/2} \quad ,$$

E_0 is the rest mass energy ($m_0 c^2$), and E_t is the total energy.

Therefore, the rms radius of the beam at the objective lens
is:

$$x_{max} = \frac{\overline{\varepsilon}_n}{\beta \gamma x'_{max}} \tag{2.74}$$

For a proton beam with kinetic energy of 100 MeV, using (2.72)
$\beta = 0.428$ and $\gamma = 1.11$.

For the case where $\overline{\varepsilon}_n = 0.01 \, \pi \times 10^{-3}$ rad cm and
$x'_{max} = 1 \, \mu$ radians, using Eq. (2.73), we have

$$x_{max} = \frac{0.01\pi \times 10^{-3} \text{ rad cm}}{\pi(.428)(1.11) \, 1 \times 10^{-6} \text{ rad}} = 21 \text{ cm}$$

For a Gaussian beam the rms radius contains 63% of the beam
intensity and a beam radius of $2x_{max}$ ($\simeq$ 42 cm) would contain 90%
of the beam intensity.

If the effect of the momentum spread is added to the
divergence, the spot size dependence on the geometric and beam
parameters can be seen. The relationship between the angular
spread and the momentum spread can be written to first order as

$$\frac{\Delta\phi}{\phi} = \frac{\Delta p_z}{p_z}$$ (2.75)

To obtain this relationship, we consider two particles with momentum p and p + Δp in the direction of propagation as shown in Fig. 17. The angle of the trajectory of the first particle with respect to the propagation direction is φ and the second is φ + Δφ.
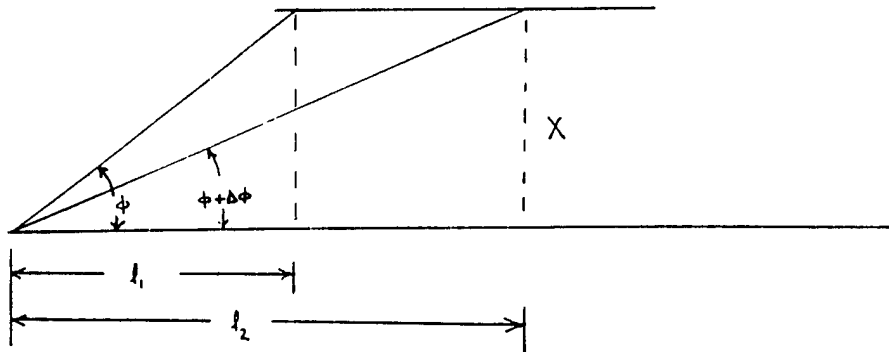
Figure 17. Figure showing the relationship between momentum and angle

In time Δt the particles will move a distance ℓ_1 and ℓ_2 in the beam direction where

$$\ell_1 = p_z \Delta t/m$$ (2.76)

$$\ell_2 = (p_z + \Delta p_z)\Delta t/m$$

Both particles have the same transverse velocity so they will

travel a distance X in the transverse direction in time Δt. The angles that each makes with the central trajectory can be written

$$\tan \phi = X/(p_z \Delta t/m)$$

(2.77)

$$\tan (\phi - \Delta\phi) = X/\big((p_z + \Delta p_z)\Delta t/m\big)$$

For small angles $\tan \phi \approx \phi$, thus

$$\phi \approx Xm/p\Delta t$$

$$\phi - \Delta\phi \approx \frac{Xm}{p_z \Delta t}\Big(\frac{1}{1 + \Delta p_z/p_z}\Big) = \phi \Big(\frac{1}{1 + \Delta p_z/p_z}\Big)$$

Therefore, $\Delta\phi = -\phi(\Delta p_z/p_z)$ or $-\Delta\phi/\phi = \Delta p_z/p_z$. If the focal length of the objective lens is F_o, from geometry, it can be seen that $\tan \phi = x_{max}/F_o$, and so $\phi \approx x_{max}/F_o$ for small angles. The total divergence can obtained by adding the two contributions to the divergence in quadrature (the square root of the sum of the squares) to obtain an estimate of the total divergence

$$\Delta\phi_t = \big((x'_{max})^2 + (\Delta\phi)^2\big)^{1/2}$$

Thus the total divergence can be estimated by the expression,

$$\Delta\phi_t = \Big[\Big(\frac{\varepsilon}{x_{max}}\Big)^2 + \Big(\frac{x_{max}}{F_o}\Big)^2 \Big(\frac{\Delta p_z}{p_z}\Big)^2\Big]^{1/2}$$

(2.78)

The spot size r_t can be obtained geometrically using the expression

$$\tan \phi_t = r_t/D \quad .$$

48

Therefore, the radius of the spot is

$$r_t = [(\frac{\varepsilon}{x_{max}})^2 + (\frac{x_{max}}{F_0})^2 (\frac{\Delta p_z}{p_z})^2]^{1/2} D. \qquad (2.79)$$

Thus, to reduce the spot size, the focal length F_0 can be increased, the momentum spread Δp decreased, and/or the emittance decreased. Since the spot size at the objective lens, x_{max}, appears in two terms, r_t can be minimized with respect to x_{max} which occurs when x_{max} satisfies the expression

$$x^2_{max} = \overline{\varepsilon} F_0 / (\Delta p_z / p_z) \qquad (2.80)$$

If x_{max} is fixed then the largest value of $\Delta p / p$ permitted is

$$\Delta p_z / p_z = \overline{\varepsilon} F_0 / X^2_{max} \qquad (2.81)$$

If a dipole steering magnet is used to aim the beam onto the target at a deflection angle α, the angular spread is related to the momentum spread,

$$\Delta \alpha = \alpha \Delta p_z / p_z \qquad (2.82)$$

Using the same argument as was used to obtain the expression for $\Delta \phi$ and imposing the condition that $\Delta \alpha < \Delta \phi_t$, one obtains the condition that

$$\alpha_{max} < \Delta \phi_t / (\Delta p_z / p_z) \qquad (2.83)$$

Thus from Eq. (2.83), we see how the maximum steering angle α_{max} is dependent on the total divergence and the momentum spread Δp.

Single Particle Optics

3.1 Equations of Motion of a Charged Particle in an Arbitrary Magnetic Field

The procedure used to calculate the trajectory of a single charged particle as it passes through an arbitrary magnetic field will now be described. This arbitrary magnetic field could be a dipole, quadrupole, sextupole, drift space or any combination of them. Classical or relativistic mechanics and electromagnetic theory, which describes the forces on the particle, are used to derive the equations of motion, a set of second order differential equations. Since these equations are nonlinear, for some special cases they can be simplified by identifying those terms which are small and disregarding them. However, if very high precision is required or if strong nonlinear effects, such as resonances are present, it may be impossible to identify the significant terms. In many cases the only way that this identification can be made is to calculate all the nonlinear terms. Usually this is difficult both analytically and numerically.

Before deriving the equations of motion, a convenient reference point and coordinate system are needed. The design of a beam transport system is simplified if certain symmetries are maintained throughout. The coordinate system is defined by three spacial directions, one in the direction of the beam, the longitudinal direction, which is usually represented by the variable z, and two transverse directions, perpendicular to the longitudinal, and perpendicular to one another. The coordinate

system is shown in Fig. 18.
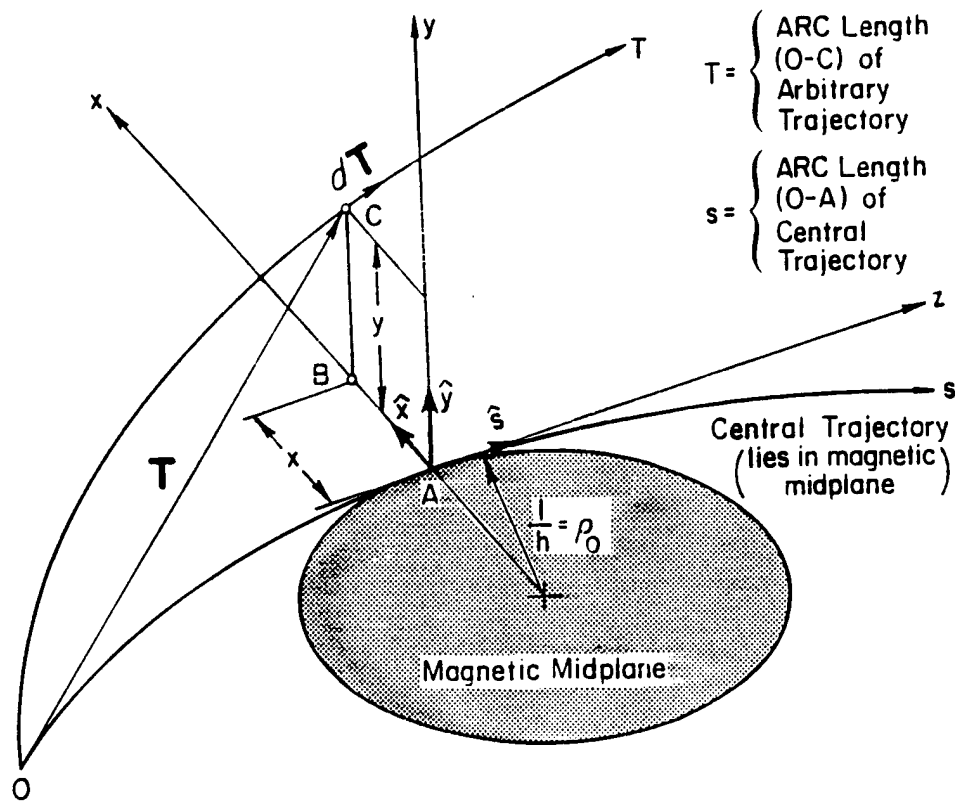
Figure 18. Curvilinear coordinate system used in the
derivation of the equations of motion
(Figure from Ref. [2])

The proper identification of the coordinate directions is
very important in identifying the direction of the magnetic
fields, the forces, and the resulting motions of particles. The
proper choice is required so vector algebra can be used and so
calculations can be simplified.

51

The concept of mid-plane symmetry and central trajectory will now be described. Consider a magnetic dipole in the shape of a ring with a gap as shown in Fig 18. With this shape the

View in Beam Direction   View From Side
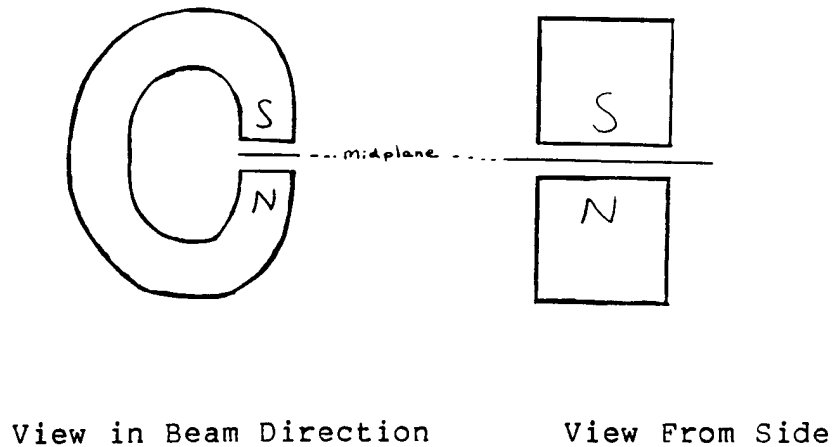
Figure 19.   A Magnetic Dipole

magnetic pole faces are opposite and parallel to one another and have a constant uniform magnetic field between them. The magnet field at the edge of the magnet, the fringe field, is not constant and therefore, it can produce significant nonlinear effects in an optical system. Since the calculation of these effects is complicated, they will not be discussed here. By arranging the magnetic optical elements in a special way, the optical design can be simplified. Starting with an imaginary plane or surface on which the design or central orbit will remain, the magnetic devices are arranged so a particle starting on the plane will remain on the plane. All the forces from external magnetic devices deflect particles on the plane along the surface of the plane. As in the magnetic dipole case, the plane on which the particle would remain, the midplane, passing through the gap in the poles, parallel to the pole faces halfway between them, as
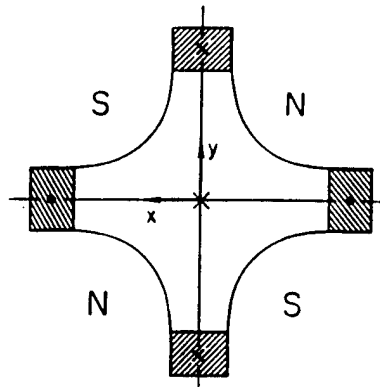
Figure 20. Outline of a quadrupole looking in the direction of the
beam (The central trajectory will pass through the
center of the quadrupole, at the intersection of the
symmetry planes. The surfaces of the quadrupole poles
are hyperboles.) (Figure from Ref. [2])

shown in Figure 19. For a quadrupole, which has two south and two

north pole faces, see Fig. 20, the midplane cuts through the center

of the quadrupole dividing it into two equal parts. Note that the

reflective (mirror like) symmetry above and below the midplane.

There are also symmetry planes at 45° to the midplane in the

quadrupole. For a pure sextupole (six poles) magnet, the midplane

lies on the symmetry plane as shown in Fig. 21.
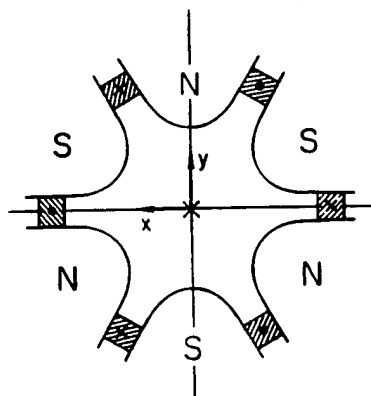
Figure 21. Sextupole magnet (Figure from Ref. [2])

The central design trajectory is the reference trajectory of a machine design. Since the trajectory is velocity dependent, particles starting with the same position and angular direction but with different velocities, will follow different trajectories. The magnetic optical elements should be arranged so the midplanes and symmetry planes of the elements, are aligned. With this arrangement, the central trajectory, defined by the beam optics, can be made to follow the geometric symmetries.

It is convenient to specify the position and velocity of a particle relative to the design or central trajectory. The coordinates are defined by the direction of the tangent line to the central trajectory at that position. We define the transverse coordinates, x and y, so by convention the x coordinate specifies displacements in the midplane and the y coordinate specifies displacements normal (perpendicular) to the midplane. Vectors oriented as shown in Fig. 18 define a right-hand curvilinear coordinate system.

With this reference line (the central trajectory) and coordinate system, the differential equations which describe the trajectories of particles near the central trajectory can now be derived. We assume that particles with trajectories that start too far from the central trajectory will be lost from the beam.

It is common for the solutions of dynamical systems to have time as the independent variable. However, for beam dynamics calculations, it is convenient to use the distance along the central trajectory as the independent variable. Thus all the time derivatives are converted to derivatives with respect to the arc

length s along the central trajectory relative to an arbitrary origin on the central trajectory. Any point of the midplane can now be uniquely defined. The y coordinate is the shortest distance to the midplane, the line segment BC, Fig. 21, is perpendicular to the midplane. The x coordinate is the shortest distance from the intersection of this line segment with the midpoint at B to the central trajectory at A. The line segment, BA, is perpendicular to the tanget line of the central trajectory at the point of intersection, A. The intersection point with the central trajectory determines the distance from the origin to the intersection point, labeled A in Fig. 21. The coordinate system shows the relative orientation of the unit vectors $\hat{x}$, $\hat{y}$ and $\hat{s}$.

The procedure for determining the equations of motion of a particle in a magnet is quite complicated. Ref. [2] contains a more detailed explanation than is presented here. We start with the Lorentz force, $\dot{p} = e(\vec{v} \times \vec{B})$, in terms of the new variables, x,y,s. Electromagmetic theory (the Laplace equation) is then used to express the magnetic field components in series in x, y and the normal derivations of the magnetic field at the central trajectory. Here it is assumed that the magnetic field can be expanded in a power series, however, this condition is not always satisfied. The differential equations for x and y written explicitly to second order (terms which have the sum of the exponents of x,y,$\dot{x}$,$\dot{y}$ and δ less than or equal to two) are

$$x'' + (1-n)h^2x = h\delta + (2n-1-\beta)h^3x^2 + h'xx' + 1/2hx'^2$$

$$+ (2-h)h^2x\delta + 1/2(h'' - nh^3 + 2\beta h^3)y^2 \qquad (3.1)$$

$$+ h'yy' - 1/2hy'^2 - h\delta^2 + \text{higher order terms}$$

$$y'' + nh^2y = 2(\beta-n)h^3xy + h'ny' - h'x'y + hx'y' + nh^2y\delta$$

$$+ \text{higher order terms}$$

where $n = - [\frac{1}{hB_y} (\frac{\partial B_y}{\partial x})]_{\substack{x=o \\ y=o}}$, $\beta = [\frac{1}{2!h^2B_y} (\frac{\partial^2 B_y}{\partial x^2})]_{\substack{x=o \\ y=o}}$,

$h = \frac{e}{p_o} B_y(o,o,\delta)$, is the radius of curvature, $\delta = \Delta p/p_o$, is the

fractional momentum deviation of the ray from that of the central

trajectory, e is the electric charge of the particle, and B_y is the

y component of the magnetic field.

Eqs. (3.1) are nonlinear equations since the right-hand sides

contain terms with more than one variable. In general, it is

difficult if not impossible to solve nonlinear equations analytically.

This is true even for the simplest equations. We will not attempt to

solve the general equations here. Instead we choose to "linearize"

them and treat the nonlinear terms as perturbations. This procedure

is referred to as a perturbative method. It will provide only a good

approximation to the actual motion or trajectory if the effects of the

higher order nonlinear terms are small. If they are not small, the

approximation is useless. Thus we are assuming that the behavior of

particles with trajectories near to the central trajectory can be predicted using the perturbative method. Note that the coordinate system has already been defined to conform to this assumption.

As an example of where this assumption fails, consider the case of an oscillatory system driven by a small periodic force whose frequency of oscillation is the same as the frequency of the oscillation of the system. In this case, the small force will drive the amplitude of the oscillator higher and higher. The amplitude will be limited by the nonlinearities of the oscillator and the relationship between the amplitude and frequency. When the frequency of the oscillation and the frequency of the driving force are multiples of one another the effect is called resonance. Thus through resonance a small force can produce a large effect. For general nonlinear systems, the relationship between the amplitude of the motion and the frequency of oscillation is quite complicated. In circular accelerators, in which particles circulate periodically, the avoidance of resonances is an important design consideration. For beam transport in the non-circulating case, it is less important because there is much less time for the resonances to develop.

To find a solution to the general equations of motion for an arbitrary charged particle, we know that the final answer will depend on the initial values of x, y, x', y' and δ. For the central trajectory, they are all zero. We assume that the general solution can be expressed as a Taylor expansion in the five variables as:

$$x = \sum_{\kappa,\lambda,\mu,\nu,\chi} (x|x_o^\kappa y_o^\lambda x_o'^\mu y_o'^\nu \delta^\chi)\ x_o^\kappa y_o^\lambda x_o'^\mu y_o'^\nu \delta^\chi$$

$$y = \sum_{\kappa,\lambda,\mu,\nu,\chi} (y|x_o^\kappa y_o^\lambda x_o'^\mu y_o'^\nu \delta^\chi)\ x_o^\kappa y_o^\lambda x_o'^\mu y_o'^\nu \delta^\chi \tag{3.2}$$

The expressions in parentheses in Eq. (3.2) are the Taylor coefficients which are determined using the equations of motion. From midplane symmetry, the following coefficients are zero:

$$(x|1) = (y|1) = 0$$

$$(x|y_o) = (y|x_o) = 0 \tag{3.3}$$

$$(x|y_o') = (y|x_o') = 0$$

To simplify the expressions for x and y, we retain only terms through second order. To this order, they can be written

$$x = c_x x_o + s_x x_o' + d_x \delta + (x|x_o^2)\ x_o^2 + (x|x_o x_o')\ x_o x_o'$$

$$+ (x|x_o\delta)\ x_o\delta + (x|x_o'^2)\ x_o'^2 + (x|x_o'\delta)\ x_o'\delta + (x|\delta^2)\delta^2 \tag{3.4a}$$

$$+ (x|y_o^2)\ y_o^2 + (x|y_o y_o')\ y_o y_o' + (x|y_o'^2)\ y_o'^2$$

and

$$y = c_y y_o + s_x y_o'$$

$$+ (y|x_o y_o)\ x_o y_o + (y|x_o y_o')\ x_o y_o' + (y|x_o' y_o)\ x_o' y_o \tag{3.4b}$$

$$+ (y|x_o' y_o')\ x_o' y_o' + (y|y_o\delta)\ y_o\delta + (y|y_o'\delta)\ y_o'\delta$$

where $c_x \equiv (x|x_o)$, $s_x \equiv (x|x_o')$, $d_x(s) \equiv (x|\delta)$, $c_y \equiv (y|y_o)$

and $s_y \equiv (y|y_o')$.

Note that the primes indicate derivatives with respect to s not time. Keeping only the first order terms of Eq. (3.4), we obtain the linear equations

$$x'' + (1-n) h^2 x = h\delta$$

$$y'' + nh^2 y = 0$$

(3.5)

Note that the y equation does not depend on the momentum deviation δ as does the x equation. The y equation describes simple harmonic oscillation through the median plane. Its solution is

$$y(s) = A \sin (\sqrt{n}hs + \phi)$$

(3.6)

where A and ϕ are determined from the initial conditions. The motion in the x directon is also a simple harmonic oscillation but the equilibrium point varies as a function of δ

$$x(s) = A \sin (\sqrt{1-n}hs + \phi) + \delta/(1-n)h$$

(3.7)

To obtain the equations of motion to second order for the case where there is no constant (dipole) term, we let $k_1 = -nh^2$ and take the limit $h \to o$, $h' \to o$, and $h'' \to o$ in Eq. (3.4). This produces the equations for a pure quadrupole field

$$x'' + k_1 x = k_1 x \delta$$

$$y'' - k_1 y = - k_1 y \delta$$

(3.8)

59

where $k_1 = B_0 e/a\rho_0$, a is the radial distance to the pole from the central trajectory, ρ_0 is the curvature of the central trajectory, and B_0/a is the magnetic field gradient.

If we let $\beta h^3 = k_2$ in Eq. (3.4) and take the limit $h \to o$, $h' \to o$, and $h'' \to o$, we obtain the equations for the perfect sextupole

$$x'' + k_2(x^2 - y^2) = 0$$

$$y'' - 2k_2 xy = 0$$

(3.9)

where

$$k_2 \equiv B_0 e/a^2 \rho_0$$

In general, the substitution of the expressions for x and y into the equations of motion gives an infinite set of second order differential equations. The first order equations in x and y are monoenergetic, only one energy, and can be written

$$c_x'' + k_x^2 c_x = 0 \quad , \qquad\qquad c_y'' + k_y^2 c_y = 0$$

(3.10)

$$s_x'' + k_x^2 s_x = 0 \quad , \qquad\qquad s_y'' + k_y^2 s_y = 0$$

where $k_x^2 \equiv (1-n)h^2$ and $k_y^2 = nh^2$, and c_x, s_x and c_y, s_y represent the two solutions. The first order equation for the dispersion, δ, is

$$d_x'' + k_x^2 d_x = \delta$$

(3.11)

The second order coefficients which represent the contributions to the second order aberrations (deviation from the linear result) have the form

$$q_x'' + k_x^2 q_x = f_x \quad , \quad q_y'' + k_y^2 q_y = f_y \tag{3.12}$$

where q_x represents the second order coefficients and f_x represents the driving terms which are treated as perturbations and whose order is one less than the order of q. For example, if $q_{x_o} = (x|x_o x_o')$ then the expression for f_x is

$$f_x = 2(2n-1-\beta)h^3 c_x s_x + h'(c_x s_x' + c_x' s_x) + h c_x' s_x' \tag{3.13}$$

which contains products of the first order solution c_x, c_x', s_x, and s_x'.

This whole procedure is confused by the large number of terms and the infinite number of equations. Obviously this procedure is useful only if the series for x and y converge very rapidly. For those cases where the series do not converge or converge slowly this procedure cannot be used.

The purpose of calculating the equations of motion for the general magnetic field has been to show the relationship between the nonlinear form of the equations and the types of aberrations that occur in a general system. Terms that contain only x_o, y_o, x_o', and y_o' produce geometric aberrations, whose order is the sum of the powers of these variable. Terms that depend on δ, the dispersion, produce chromatic aberrations.

61

3.2 First Order Optics

To design a beam optical system, the first order dynamics must be calculated first. Later refinements can be made to include or reduce higher order effects. Since the relationship between the beam variables to first order are linear, it is convenient to use linear maps as described in section 2.3. It is possible to calculate the dynamical variables, positions and velocities of a beam particle as it exits an optical element if its entry values are known. Mathematically this means that the expressions for the final values do not contain terms with more than one entry variable. To simplify the notation as was introduced in section 2.3, we use a convention that denotes the variable by subscripts (elements of a vector) x_1, x_2, x_3, x_4, x_5, x_6 in place of separate labels x, x', y, y', ℓ, δ. For the linear case this can be written in the mathematical short hand

$$x_f = \sum_{i=1}^{6} R_{fi} \, x_i \qquad f = 1,2,\ldots,6 \qquad (3.14)$$

where the x_f are the final (exit) variable and x_i are the initial (entry) variables and the $R_{fi} = (x_f, x_i)$. In matrix notation it can be written

$$x_f = Rx_i \qquad (3.15)$$

The matrix R is a linear mapping of the entry variable values to the exit variable values as was introduced in section 2.3. Recall that some of the matrix elements are zero because of midplane symmetry. In general the matrix R can be written

$$R = \begin{pmatrix} c_x(s) & s_x(s) & 0 & 0 & 0 & d_x(s) \\ c'_x(s) & s'_x(s) & 0 & 0 & 0 & d'_x(s) \\ 0 & 0 & c_y(s) & s_y(s) & 0 & 0 \\ 0 & 0 & c'_y(s) & s'_y(s) & 0 & 0 \\ R_{51} & R_{52} & R_{53} & R_{54} & R_{55} & R_{56} \\ R_{61} & R_{62} & R_{63} & R_{64} & R_{65} & R_{66} \end{pmatrix} \quad (3.16)$$

If one of the subscripts of the matrix element R_{fi} is a six then the term containing that element is called a chromatic term, since it would multiply with the δ (or x_6) variable which is the fractional deviation from the reference momentum, the momentum spread. These are called chromatic because they depend on energy differences. In light optics different colors of light have different wavelengths and behave differently in optical systems. These color effects are referred to as chromatic. Terms containing matrix elements that do not contain a six as a subscript are called geometric terms.

If the study of particle dynamics is restricted to particles having the reference momentum ($\delta = 0$), no chromatic terms, then the 6x6 R matrix can be reduced to two 2x2 matrices, one for each transverse direction. The 4 x 4 matrix

$$R = \begin{pmatrix} c_x(s) & s_x(s) & 0 & 0 \\ c'_x(s) & s'_x(s) & 0 & 0 \\ 0 & 0 & c_y(s) & s_y(s) \\ 0 & 0 & c'_y(s) & s'_y(s) \end{pmatrix} \quad (3.17)$$

$$R = \begin{pmatrix} D_x & 0 \\ 0 & D_y \end{pmatrix} \qquad (3.18)$$

where D_x and D_y are 2x2 matrices

$$D_x = \begin{pmatrix} c_x(s) & s_x(s) \\ c_x'(s) & s_x'(s) \end{pmatrix}$$

$$\qquad (3.19)$$

$$D_y = \begin{pmatrix} c_y(s) & s_y(s) \\ c_y'(s) & s_y'(s) \end{pmatrix}$$

In this case the two transverse directions are uncoupled, i.e. the motion in the two planes are independent.

For this simplified condition, it is possible to construct the transfer matrices for simple beam elements and combine them using matrix multiplication to obtain the transfer matrix for the transport system.

3.3 Drift Space

The transfer matrix for free drift space of length L, which contains no external electric and magnetic fields is

$$R = \begin{pmatrix} 1 & L \\ 0 & 1 \end{pmatrix} \qquad (3.20)$$

If the position and angle of the drift space are x_1, x_1' at the beginning, and x_2, x_2' at the end, as shown in Fig. 22, then

64

$$
\begin{pmatrix} x_2 \\ x_2' \end{pmatrix} = \begin{pmatrix} 0 & \ell \\ 0 & 1 \end{pmatrix} \begin{pmatrix} x_1 \\ x_1' \end{pmatrix} \tag{3.21}
$$

so that

$$
\Delta x = x_2 - x_1 = L x_1' \tag{3.22}
$$

$$
x_2' = x_1' = \text{constant}
$$
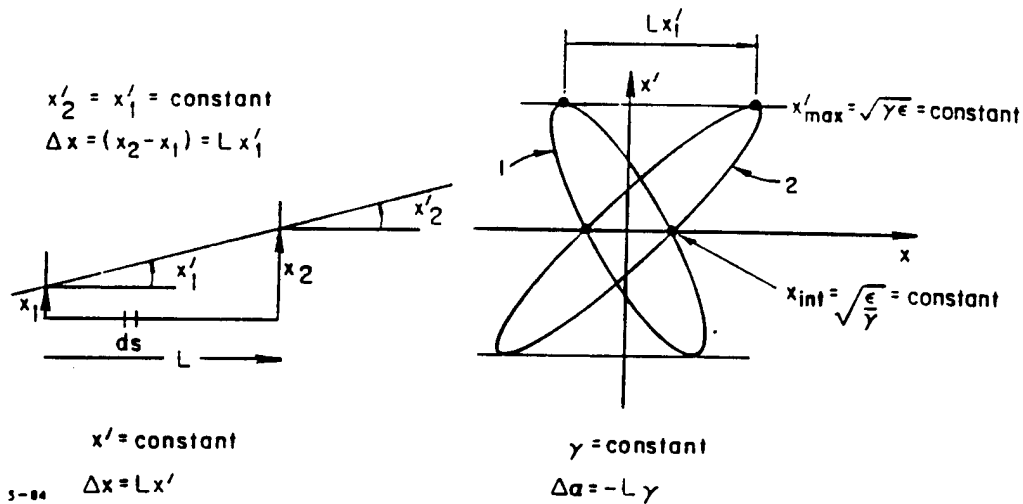
Figure 22. The transformation of a beam ellipse through a drift (field-free) space (Figure from Ref. [2])

The beam ellipse evolves so x' and x intercepts remain constant as shown in Fig. 22. Over a long drift space the ellipse can become elongated corresponding to a spreading of the beam. See section 2.9 for a discussion of the beam ellipse.

3.4 Thin Lens

We have shown in the previous section that a drift space changes only the position and not the angle. When the transfer matrix for a thin lens is calculated, it is found to change the

65

angle but not the position. Consider the transfer matrix for a thin lens

$$R = \begin{pmatrix} 1 & 0 \\ -1/F & 1 \end{pmatrix} \tag{3.23}$$

then

$$\begin{pmatrix} x_2 \\ x_2' \end{pmatrix} = \begin{pmatrix} 1 & 0 \\ -1/F & 1 \end{pmatrix} \begin{pmatrix} x_1 \\ x_1' \end{pmatrix} \tag{3.24}$$

The matrix multiplication gives the equations

$$x_2 = x_1$$
$$\tag{3.25}$$
$$x_2' = x_1' - x_1/F$$

Thus matrix R does not change the position but changes the angle proportional to the displacement x_1.

With this angular deflection, a particle traveling parallel to the reference trajectory at a distance x_1 ($x_i = 0$) will be deflected
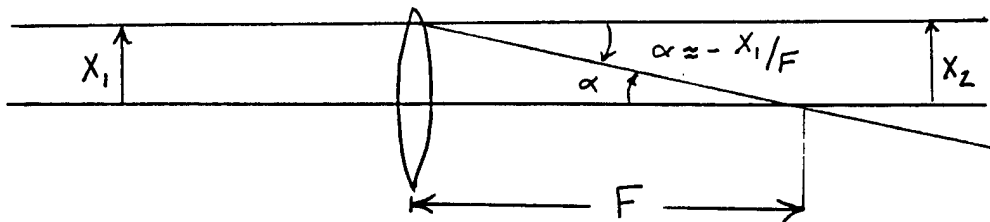
Figure 23. The transformation of a beam ellipse through a focusing thin lens (Figure from Ref. [2])

towards the reference trajectory, as shown in Fig. 23, and intersect it at a distance F, so that $\tan\alpha$ ($\approx\alpha$) = $-x_1/F$. The matrix R corresponds to a focusing lens of focal length F. The beam ellipse of a focusing lens is shown in Fig. 24.

66
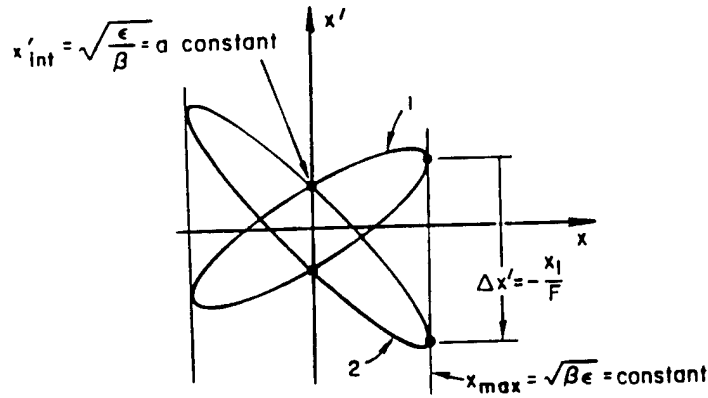
Figure 24. The beam ellipse of a focusing lens
(Figure from Ref. [2])

In the case where $x_1 = x_2$, the points where the initial beam ellipse crosses the x' axis are the same as the points where all final beam ellipses cross the x' axis regardless of the focal length F. If F is small, the angular change is large and the beam ellipse will become very long and narrow. A very short focal length will produce a large angular spread in the beam.

A very thin quadrupole lens acts like a thin lens, but it focuses in one plane and defocuses in the other plane. Fig. 25 shows a diagram of the fields of a quadrupole. If the transfer matrix in the (x,x') plane is focusing, then

$$R_x = \begin{pmatrix} 1 & 0 \\ -1/F & 1 \end{pmatrix} \tag{3.26}$$

and the transfer matrix in the (y,y') plane will be defocusing

$$R_y = \begin{pmatrix} 1 & 0 \\ +1/F & 1 \end{pmatrix} \tag{3.27}$$

67
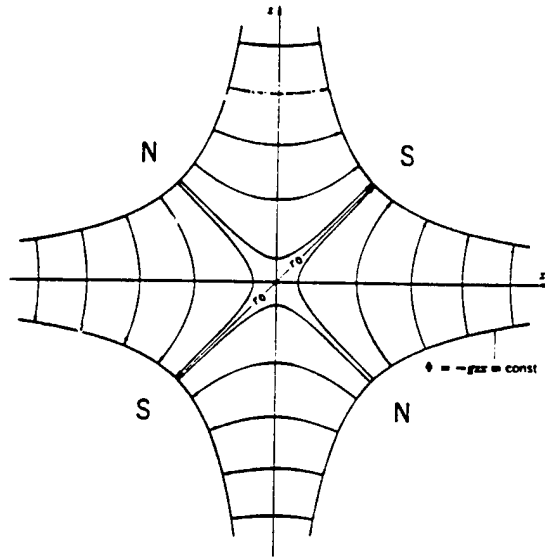
Figure 25. Magnetic fields lines of a quadrupole
(Figure from Ref. [2])

3.5 Composite System of a Thin Lens with Two Drift Spaces

We can now construct a simple composite system consisting of two
drift spaces and a thin lens with a focal length F, as shown in
Fig. 26.
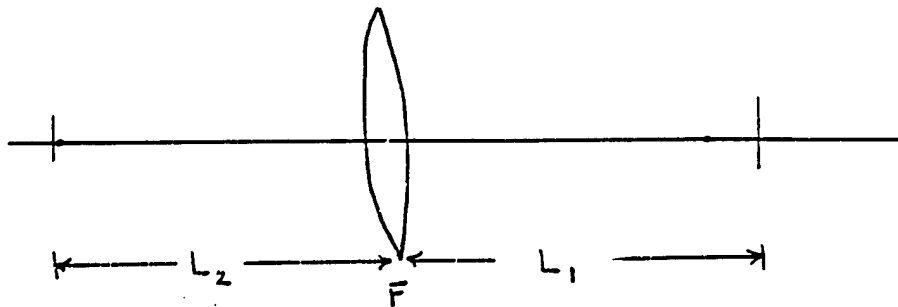
Figure 26. Composite system, two drifts and a thin lens

$$R = \begin{pmatrix} 1 & L_1 \\ 0 & 1 \end{pmatrix} \begin{pmatrix} 1 & 0 \\ -1/F & 1 \end{pmatrix} \begin{pmatrix} 1 & L_2 \\ 0 & 1 \end{pmatrix} \qquad (3.28)$$

To multiply two matrices together, recall that

$$P = \begin{pmatrix} a_{11} & a_{12} \\ a_{21} & a_{22} \end{pmatrix} \begin{pmatrix} b_{11} & b_{12} \\ b_{21} & b_{22} \end{pmatrix}$$

$$(3.29)$$

$$P = \begin{pmatrix} a_{11}b_{11} + a_{12}b_{21} & a_{11}b_{12} + a_{12}a_{22} \\ a_{21}b_{11} + a_{21}b_{21} & a_{21}b_{12} + a_{22}b_{22} \end{pmatrix}$$

Repeating the above multiplication procedure on the above matrix, we have

$$R = \begin{pmatrix} 1 & L_1 \\ 0 & 1 \end{pmatrix} \begin{pmatrix} 1 & L_2 \\ -1/F & 1-L_2/F \end{pmatrix} \qquad (3.30)$$

$$R = \begin{pmatrix} 1-L_1/F & L_2+L_1(1-L_2/F) \\ -1/F & 1-L_2/F \end{pmatrix} \qquad (3.31)$$

If the drift lengths are selected to be equal to the focal length, then the R matrix is reduced to

69

$$R = \begin{pmatrix} 0 & F \\ -1/F & 0 \end{pmatrix} \qquad (3.32)$$

In this case we see that angles are converted to displacements and displacements to angles, by using Eq. (3.32) to calculate x_2 and x_2'. Thus

$$x_2 = Fx_1' \qquad (3.33)$$

$$x_2' = -x_1/F$$

To obtain net focusing in the two transverse directions, it is necessary to have either a quadrupole triplet or quadruplet.

3.6 Magnetic Quadrupole Lens

The concept of building an optical system using transfer matrices has been demonstrated and we have shown how they can combine to produce a single transfer matrix. We are ready to calculate the transfer matrix of a quadrupole lens for particles moving at the design energy ($\delta = 0$). By using Eqs. (3.5) for $\delta = 0$, we have the equations of motion for a particle in a quadrupole field as

$$\frac{dx^2}{ds^2} = kx$$

$$\frac{dy^2}{ds^2} = ky \qquad (3.34)$$

70

where $k \equiv (qB_O/\gamma m_O a v_S)$, with q the particle charge, B_O/a the magnetic field gradient, γm_O the relativistic mass and v_S the longitudinal velocity. The solutions to Eq. (3.34) are

$$x(s) = x_1 \cos(\sqrt{k}\ s) + x_1' \sin(\sqrt{k}\ s)/\sqrt{k}$$

$$x'(s) = -x_1\ \sqrt{k}\ \sin(\sqrt{k}\ s) + x_1' \cos(\sqrt{k}\ s)$$

$$(3.35)$$

$$y(s) = y_1 \cosh(\sqrt{k}\ s) + y_1' \sinh(\sqrt{k}\ s)/\sqrt{k}$$

$$y'(s) = y_1\ \sqrt{k}\ \sinh(\sqrt{k}\ s) + y_1' \cosh(\sqrt{k}\ s)$$

where s denotes the location along the central orbit, B_O is the magnitude of the magnetic field at the surface of the pole closest to the axis and a is the minimum distance from the center to the pole face.

The transfer matrix in the (x,x') plane can be written for the focusing case of a quadrupole lens of length ℓ as

$$R_x^F = \begin{pmatrix} \cos\Gamma & \sin\Gamma/\sqrt{k} \\ -\sqrt{k}\ \sin\Gamma & \cos\Gamma \end{pmatrix} \qquad (3.36)$$

and for the defocusing case

$$R_x^D = \begin{pmatrix} \cosh\Gamma & \sinh\Gamma/\sqrt{k} \\ \sqrt{k}\ \sinh\Gamma & \cosh\Gamma \end{pmatrix} \qquad (3.37)$$

71

where $\Gamma \equiv \sqrt{k}\ \ell$. Since most quadrupole lens have $\Gamma \leqslant 1$, it is possible to expand the cosine, sine, hyperbolic sine and cosine in a power series in Γ to obtain

$$
R_x^F = \begin{pmatrix} 1 - \Gamma^2/2 + \Gamma^4/24 & (\Gamma - \Gamma^3/6 + \ldots)/\sqrt{k} \\[2ex] -\sqrt{k}\,(\Gamma - \Gamma^3/6 + \ldots) & 1 - \Gamma^2/2 + \Gamma^4/24 + \ldots \end{pmatrix}
$$

$$(3.38)$$

$$
R_x^D = \begin{pmatrix} 1 + \Gamma^2/2 + \Gamma^4/24 & (\Gamma + \Gamma^3/6 + \ldots)/\sqrt{k} \\[2ex] \sqrt{k}\,(\Gamma + \Gamma^3/6 + \ldots) & 1 + \Gamma^2/2 + \Gamma^4/24 + \ldots \end{pmatrix}
$$

If only the first order terms are retained as $\ell \to 0$, we obtain the thin lens matrices of (3.26) and (3.27) for $F = 1/k\ell$.

We are now ready to investigate the focusing of a system of quadrupole lens, a doublet, a triplet and a quadruplet. The triplet and quadruplet are candidates for the objective lens of a telescope and the triplet is used for the eyepiece. Quadrupole lens form the basis of most transport systems. They are used for focusing in an achromatic bend for example. This will be discussed later.

Starting with a quadrupole doublet, we assume the sequence of quadrupoles is such that in the x direction it is focusing then defocusing, and in the y direction it is defocusing then focusing. We ignore the drift space between the two quadrupoles. For the (x, x') plane the transfer matrix is

$$R^D_x R^F_x = \begin{pmatrix} \cosh\Gamma & \sinh\Gamma/\sqrt{k} \\ \\ \sqrt{k}\,\sinh\Gamma & \cosh\Gamma \end{pmatrix} \begin{pmatrix} \cos\Gamma & \sin\Gamma/\sqrt{k} \\ \\ -\sqrt{k}\,\sin\Gamma & \cos\Gamma \end{pmatrix}$$

$$(3.39)$$

$$= \begin{pmatrix} \cos\Gamma\,\cosh\Gamma - \sin\Gamma\,\sinh\Gamma & (\cosh\Gamma\,\sin\Gamma + \cos\Gamma\,\sinh\Gamma/\sqrt{k}) \\ \\ (\cos\Gamma\,\sinh\Gamma - \cosh\Gamma\,\sin\Gamma)\sqrt{k} & \cos\Gamma\,\cosh\Gamma + \sin\Gamma\,\sinh\Gamma \end{pmatrix}$$

For the (y, y') plane, the transfer matrix is

$$R^F_y R^D_y = \begin{pmatrix} \cos\Gamma\,\cosh\Gamma + \sin\Gamma\,\sinh\Gamma & (\cosh\Gamma\,\sin\Gamma + \sinh\Gamma\,\cos\Gamma)/\sqrt{k} \\ \\ (\cos\Gamma\,\sinh\Gamma - \cosh\Gamma\,\sin\Gamma)\sqrt{k} & \cos\Gamma\,\cosh\Gamma - \sin\Gamma\,\sinh\Gamma \end{pmatrix} (3.40)$$

To compare the focal lengths in the two planes, we consider the case where $x'_1 = 0$, $y'_1 = 0$ and $x_1 = y_1$. In (x, x') plane

$$x_2 = (\cos\Gamma\,\cosh\Gamma - \sinh\Gamma\,\sin\Gamma)\, x_1$$

$$(3.41)$$

$$x'_2 = (\cos\Gamma\,\sinh\Gamma - \cosh\Gamma\,\sin\Gamma)/\sqrt{k}\; x_1$$

and in the (y, y') plane:

$$y_2 = (\cos\Gamma\,\cosh\Gamma + \sinh\Gamma\,\sin\Gamma)\, y_1$$

$$(3.42)$$

$$y'_2 = (\cos\Gamma\,\sinh\Gamma - \cosh\Gamma\,\sin\Gamma)/\sqrt{k}\; y_1$$

where x_2, x'_2, y_2 and y'_2 are the values of x, x', y and y' at the end of the second quadrupole.
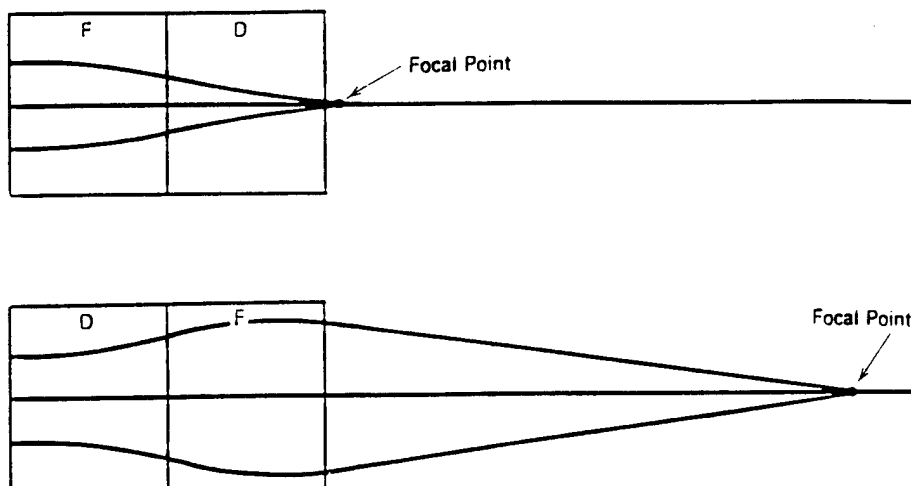
Figure 27. Sketch of the different focal lengths for the x and y planes in a quadrupole doublet (Figure from Ref. [1])

From the geometry and the definition of focal length, we see that

$$\tan x_2' = x_2/F_x$$

$$\tan y_2' = y_2/F_y$$

So that   (3.43)

$$F_x = x_2/\tan x_2'$$

$$F_y = y_2/\tan y_2'$$

From the expressions for x_2' and y_2', we see that they are equal since $x_1 = y_1$. Since $\cosh\Gamma$ and $\sinh\Gamma$ are increasing functions of Γ, the second term of the x_2 expression in Eq. (3.41) produces a value for x_2 which is less than y_2 in Eq. (3.42). Thus, F_y is greater than F_x. When a parallel beam ($x' = y' = 0$) passes through a quadrupole doublet, it is not focused to a single point but along a horizontal line. An optical system with this condition is said to be astigmatic. A system which focuses a beam to a single point is said to be stigmatic.

74

To obtain a stigmatic system, a quadrupole triplet is required. In this arrangement the first and third quadrupole have the same length, orientation, and magnetic field gradients while the second quadrupole is like the other two but is twice as long with its magnetic field gradient rotated ninety degrees with respect to the other two. Thus the first and third quadrupoles are focusing, the second is defocusing, and visa versa for the other direction.

If the drift space between the quadrupoles is ignored, it can be shown that the matrix product of individual quadrupoles in a focus, defocus, focus combination produces a total transfer matrix that can be reduced to

$$
R_{FDF} = \begin{pmatrix} \cos\Gamma_2 \, \cosh\Gamma_2 & \dfrac{1}{\sqrt{k}} \, (\cosh\Gamma_2 \, \sin\Gamma_2 + \sinh\Gamma_2) \\ \sqrt{k} \, (\sinh\Gamma_2 - \cosh\Gamma_2 \, \sin\Gamma_2) & \cosh\Gamma_2 \, \cos\Gamma_2 \end{pmatrix} \tag{3.44}
$$

For a defocus, focus, defocus combination, the total transfer matrix is

$$
R_{DFD} = \begin{pmatrix} \cos\Gamma_2 \, \cosh\Gamma_2 & \dfrac{1}{\sqrt{k}} \, (\cos\Gamma_2 \, \sinh\Gamma_2 + \sin\Gamma_2) \\ \sqrt{k} \, (\cos\Gamma_2 \, \sinh\Gamma_2 - \sin\Gamma_2) & \cos\Gamma_2 \, \cosh\Gamma_2 \end{pmatrix} \tag{3.45}
$$

If the triplet has focusing, defocusing, focusing in the (x,x') plane, then it will have defocusing, focusing, defocusing in the

(y,y') plane. Note that the off diagonal elements for R_{FDF} and R_{DFD} are not equal.
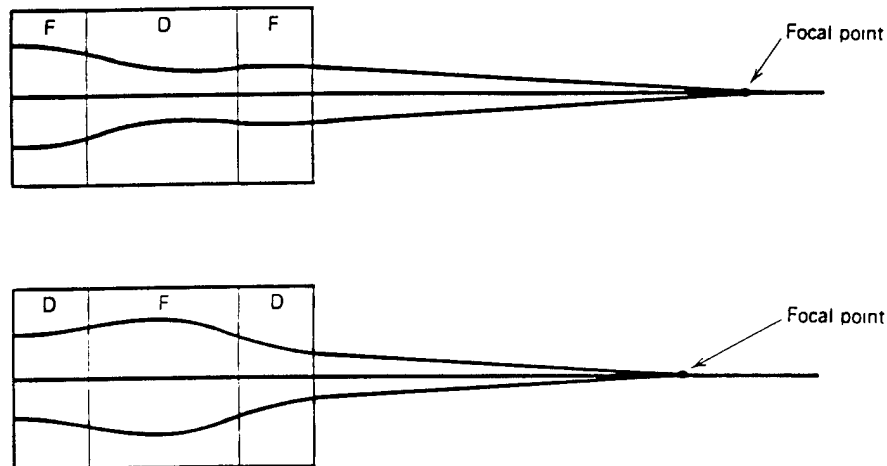
Figure 28.　Improved stigmatic properties of a quadrupole triplet
　　　　　　lens where (a) correspondes to the x plane and (b) to
　　　　　　the y plane in the example.　Orbits of particles
　　　　　　initially parallel to the axis projected in the x and
　　　　　　y planes (Figure from Ref. [1])

Figure 28 shows the effects of the quadrupole triplet in the x and
y planes. However, if the trignometric and hyperbolic functions
in the two matrices are expanded in a power series in Γ, they
reduce in the lowest order to the same simple matrix

$$R_{triplet} = \begin{pmatrix} 1 & 2\ell \\ -k^2\ell^3/6 & 1 \end{pmatrix} \qquad (3.46)$$

This demonstrates for this simple case and to this order, a
quadrupole triplet is a stigmatic device.

76

3.7 Magnetic Dipole

There is one more very useful optical element, the dipole, must be discussed before we can construct composite systems such as the 180° achromatic bend. Quadrupoles are used to focus the beam, dipoles are used to bend the beam. The tansfer matrix for a dipole is diffcult to calculate because of the curvature of the design trajectory and the corresponding change in the coordinate system as seen in Fig. 18. A sector magnet dipole is shown in Fig. 29.
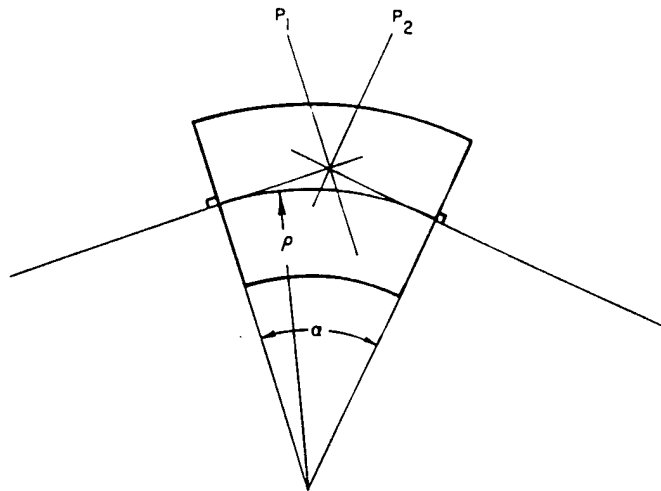
Figure 29. A sector dipole magnet (Figure from Ref. [2])

In keeping with the symmetries introduced earlier, the dipole is oriented so that the magnet poles are along the x direction with the magnetic field in the y direction. Displacements and angle are measured with respect to the reference or central trajectory as usual. We use the simplification that the magnetic field is uniform radially and fringe fields are ignored. The pole entry and exit faces are perpendicular to the reference (design trajectory) and the motion in the (x,x') and (y,y') planes are uncoupled.

77

The transfer matrix for the (x, x') plane for the linear non-dispersion case is

$$R_x = \begin{pmatrix} \cos\alpha & \rho\sin\alpha \\ -1/\rho\sin\alpha & \cos\alpha \end{pmatrix} \qquad (3.47)$$

where ρ is the radius of the central orbit and α is the sector angle of the magnet. In the vertical direction the transfer matrix is that of a drift space,

$$R_y = \begin{pmatrix} 1 & \rho\alpha \\ 0 & 1 \end{pmatrix} \qquad (3.48)$$

3.8 Second Order Optics

Second order terms as expressed in (3.4) are those that contain the product of two initial dynamical variables such as xx_o', $x_o'\delta$, etc. and the nonlinear coefficient. To use the same type of notation as was used for the linear case, a tensor T_{ijk}, is used. In this notation the coefficient $(x|x_o x_o')$ is written as

$$T_{112} \equiv (x|x_o x_o') \qquad (3.49)$$

As was the situation for the linear case, coefficients of the nonlinear terms which contain no subscripts equal to six are referred to as geometric terms and correspond to geometric aberration. Those that contain one or more subscripts equal to six are called chromatic terms and correspond to chromatic aberrations which depend on the momentum deviation $\Delta p/p$ of the particle.

$d_z = (z\|\delta)$	h		
$(z\|z_0^2)$	$+ (2n - 1 - \beta)h^3 c_z^2$	$+h'c_z c'_z$	$+\frac{1}{2}hc'^2_z$
$(z\|z_0 z'_0)$	$+2(2n - 1 - \beta)h^3 c_z s_z$	$+h'(c_z s'_z + c'_z s_z)$	$+hc'_z s'_z$
$(z\|z_0\delta)$	$(2-n)h^2 c_z \quad +2(2n-1-\beta)h^3 c_z d_z$	$+h'(c_z d'_z + c'_z d_z)$	$+hc'_z d'_z$
$(z\|z'^2_0)$	$(2n-1-\beta)h^3 s_z^2$	$+h's_z s'_z$	$+\frac{1}{2}hs'^2_z$
$(z\|z'_0\delta)$	$(2-n)h^2 s_z \quad +2(2n-1-\beta)h^3 s_z d_z$	$+h'(s_z d'_z + s'_z d_z)$	$+hs'_z d'_z$
$(z\|\delta^2)$	$-h + (2-n)h^2 d_z \quad +(2n-1-\beta)h^3 d_z^2$	$+h'd_z d'_z$	$+\frac{1}{2}hd'^2_z$
$(z\|y_0^2)$	$\frac{1}{2}(h'' - nh^3 + 2\beta h^3)c_y^2$	$+h'c_y c'_y$	$-\frac{1}{2}hc'^2_y$
$(z\|y_0 y'_0)$	$(h'' - nh^3 + 2\beta h^3)c_y s_y$	$+h'(c_y s'_y + c'_y s_y)$	$-hc'_y s'_y$
$(z\|y'^2_0)$	$\frac{1}{2}(h'' - nh^3 + 2\beta h^3)s_y^2$	$+h's_y s'_y$	$-\frac{1}{2}hs'^2_y$
$(y\|z_0 y_0)$	$2(\beta - n)h^3 c_z c_y$	$+h'(c_z c'_y - c'_z c_y)$	$+hc'_z c'_y$
$(y\|z_0 y'_0)$	$2(\beta - n)h^3 c_z s_y$	$+h'(c_z s'_y - c'_z s_y)$	$+hc'_z s'_y$
$(y\|z'_0 y_0)$	$2(\beta - n)h^3 s_z c_y$	$+h'(s_z c'_y - s'_z c_y)$	$+hs'_z c'_y$
$(y\|z'_0 y'_0)$	$2(\beta - n)h^3 s_z s_y$	$+h'(s_z s'_y - s'_z s_y)$	$+hs'_z s'_y$
$(y\|y_0\delta)$	$nh^2 c_y \quad +2(\beta - n)h^3 c_y d_z$	$-h'(c_y d'_z - c'_y d_z)$	$+hc'_y d'_z$
$(y\|y'_0\delta)$	$nh^2 s_y \quad +2(\beta - n)h^3 s_y d_z$	$-h'(s_y d'_z - s'_y d_z)$	$+hs'_y d'_z$

Table 1.   The driving terms for the nonlinear coefficients (Figure from Ref. [2])

The driving terms which produce the second order terms in a general magnet are displayed in Table I, which appears in Ref.[2]. To obtain the second order terms for a pure dipole, we let $n = 0$, $\beta = 0$ and $h = (1/\rho_0)$. For a pure quadrupole, we let $\beta = 0$, $k_1 = -(nh^2)$ and take the limit $(h) \to 0$. For a pure sextupole, we let $k_2 = Bh^3$ and take the limit $h \to 0$, $nh^2 \to 0$. By carefully studying the tables of Ref. [2] with these conditions, one can see that a pure dipole produces both second order geometric and chromatic aberrations, that a quadrupole to second order does not produce geometric aberrations but it does produce chromatic aberrations, and that a sextupole produces to second order both geometric and chromatic aberrations.

3.9 Aberrations in Magnetic Quadrupole Lens System

In this subsection, analytic expressions for third order (spherical) aberrations in a magnetic quadrupole lens system are developed. It is a summary of a paper by R. W. Moses, E. A. Heighway, R. S. Christian and A. J. Dragt titled, "Scaling Laws for Aberrations in Magnetic Quadrupole Lens Systems," Ref. [8]. Some of what is presented here is not new to that paper, but was contained in much earlier articles and books sited as references in that paper. It contains a comparison of the analytical description and numerical integration of the quadrupole doublet and triple lens systems. Embedded magnetic octupoles are used to reduce third order aberrations according to analytic predictions.

It was shown by Moses (1966) that no combination of electro-static and magnetic quadrupoles will result in the elimination of third order spherical aberrations. However, it is possible to reduce or eliminate these third order aberrations using quadrupoles and octupoles. In Ref. [8], simple analytic approximations of quadrupole aberrations and octupole corrections are obtained which can be used as a guide in designing these systems. Their equations are reproduced here to illustrate the method. The reader is encouraged to read the paper for additional details and discussion.

As usual, the linear properties of the system are derived first. The vacuum magnetic fields for quadrupoles and octupoles are given in terms of scalar magnetic potentials V_Q and V_O for the quadrupoles and octupoles as

$$\vec{B} = -\nabla V_Q - \nabla V_O \quad . \tag{3.50}$$

80

The magnetic scalar potentials are given by the equations

$$(e/p) \ V_Q = - xy\phi(z) + xy(x^2 + y^2) \ \phi''/12 + \ldots$$

$$(3.51)$$

$$(e/p) \ V_O = - xy \ (x^2 - y^2) \ \psi/3 + \ldots$$

where e and p are the charge and magnitude of the momentum of the particle and $\phi(z)$, $\psi(z)$ are the quadrupole and octupole gradient functions.

As we have seen earlier, in Eq. (3.5), the paraxial equations are obtained when only the linear terms are retained. They can be written

$$x'' + \phi(z)x = 0$$

$$(3.52)$$

$$y'' - \phi(z)y = 0$$

The prime indicates derivatives with respect to z. The general solution to these equations can be written in terms of the initial conditions x_0, y_0, x_0' and y_0' at z_0 as

$$x(z) = x_0 c_x(z) + x_0' s_x(z)$$

$$(3.53)$$

$$y(z) = y_0 c_y(z) + y_0' s_y(z)$$

where c_x, c_y, s_x and s_y are the paraxial solutions with initial conditions

$$c_x(z_0) = c_y(z_0) = s_x'(z_0) = s_y'(z_0) = 1 \quad ,$$

$$(3.54)$$

$$c_x'(z_0) = c_y'(z_0) = s_x(z_0) = s_y(z_0) = 0 \quad .$$

The solutions of the general equations through third order can be written, see Eq. (3.2), with the assumption that x_0 and y_0 are small and so the nonlinear terms involving x_0 and y_0 can be ignored,

$$x_i \simeq (x|x_0)x_0 + (x|x_0'x_0'x_0')x_0'^3 + (x|x_0'y_0'y_0')\ x_0'y_0'^2$$

$$(3.55)$$

$$\simeq m_x\ (x_0 + C_1 x_0'^3 + C_2 x_0'y_0'^2)$$

and

$$y_i \simeq (y|y_0)y_0 + (y|y_0'^3)y_0'^3 + (y|x_0'x_0'y_0')\ x_0'^2 y_0'$$

$$(3.56)$$

$$\simeq m_y\ (y_0 + D_1 y_0'^3 + D_2 x_0'^2 y_0')$$

where m_x and m_y are the linear magnification factors. The coefficients C_1, C_2, D_1 and D_2 can be reduced to the following form:

$$C_1 = \int_{z_0}^{z_i} [c_x'^4/6 + (\phi^2 + \psi)\ c_x^4/3]\ dz$$

$$C_2 = D_2 = \int_{z_0}^{z_i} [1.5 c_x'^2 c_y'^2 + (\phi^2 - \psi)\ c_x^2\ c_y^2]\ dz \qquad (3.57)$$

$$D_1 = \int_{z_0}^{z_i} [c_y'^4/6 + (\phi^2 + \psi)\ c_y^4/3]\ dz$$

The observation that the integrals are positive definite (contain terms which are even powers of c_x, c_y, c_x' and c_y' and are positive), implies that it is impossible in this approximation to have these

82

coefficients equal to zero using quadrupoles alone ($\psi = 0$).

3.10 Quadrupole Doublet

The analytic expressions for the third order aberrations of the quadrupole doublet, shown in Fig. 30, are presented by Moses et al in Ref. [8]. They are reproduced here for illustration. The x and y trajectories have a common object plane z_o and are focused to a virtual image at infinity. Quantities are defined as they appear in Fig. 30.
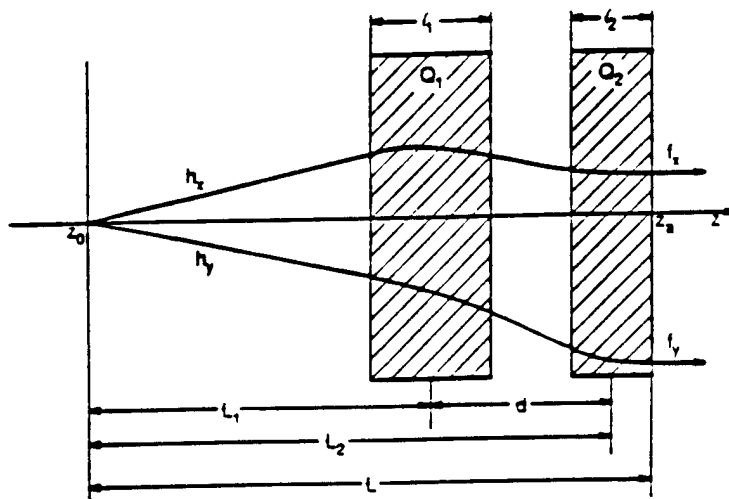

Figure 30. Schematic description of a quadrupole doublet
(Figure from Ref. [8])

The total focal length of the system in each coordinate (x and y) is given by the formula (obtain using the linear matrix method described earlier in this section),

$$\frac{1}{f_{x,y}} \simeq \frac{1}{f_{x,y1}} + \frac{1}{f_{x,y2}} - d/(f_{x,y1} \, f_{x,y2}) \tag{3.58}$$

where

$$f_{x,yn} \equiv F_{x,yn}/[1 - \ell_n/(6F_{x,yn})] \tag{3.59}$$

and

$$F_{xn} \equiv - F_{yn} = 1/\phi_n \ell_n \qquad . \tag{3.60}$$

The subscript x,yn refers to either the x or y coordinate.
Eq. (3.59) corresponds to Eq. (3.38) for the approximation of the
quadrupole lens. The ϕ_n of Eq. (3.60) is the quadrupole gradient
function for each quadrupole. Within the drift space $\phi_n = 0$.

Moses et al claim that for this system F_{x2}, F_{x1}, $f_{x,y}$ can be
approximated by the expression

$$F_{x2} \simeq - \{dL_2[1 - (L_2\ell_2/L_1 + \ell_2)/6d]\}^{1/2} \tag{3.61}$$

$$F_{x1} \simeq - F_{x2} \, L_1/L_2 \tag{3.62}$$

$$f_{x,y} = L_1/(1 - df_{x,y2}) \tag{3.63}$$

The aperture aberration coefficients of a doublet can be
approximated by the expression

$$C_1 \simeq [L_1 + (f_x - L_1)^4/d^3]/6 + [L_1^4/(\ell_1 f_{x1}^2) + f_x^4/(\ell_2 f_{x2}^2)]/3 \tag{3.64a}$$

$$C_2 = D_2 \simeq 1.5[L_1 + (f_x - L_1)^2 (f_y - L_1)^2/d^3] + L_1^4/(\ell_1 f_{x1} f_{y1})$$
$$+ f_x^2 f_y^2/(\ell_2 f_{x2} f_{y2}) \tag{3.64b}$$

$$D_1 \simeq [L_1 + (f_y - L_1)^4/d^3]/6 + [L_1^4/(\ell_1 f_{y1})^2 + f_y^4/(\ell_2 f_{y2})^2]/3 \tag{3.64c}$$

These expressions have not been verified by this author. This clearly shows that it is difficult to see the relationships between aberration coefficients and the design parameters even for this simple case.

The results from these analytic expressions were compared with the numerical results of the computer codes MARYLIE and GIOS. The agreement is excellent for the case of equal length quadrupoles which occupy less than half the length L. If the quadrupoles are of different lengths and short, the agreement is still good. When they are of very different lengths and occupy half of L, the errors are much larger.

The quadrupole triplet case was not calculated in general. By using two mirror image doublets, a symmetrical approximation to a triplet was obtained by Moses et al. A numerical example showed good agreement with these analytical results.

The octupole aberration correction was not present in this paper. Reference was made to an earlier paper by Moses, Ref. [9]. It is claimed that at least three octupoles ideally centered are needed to completely correct the third-order aberrations and that for miminum strength octupoles the inequalities

$$(c_x/c_y)_b^2 > (c_x/c_y)_c^2 > (c_x/c_y)_d^2$$

should be maximized, with the sign of $\psi(z_b)$ and $\psi(z_d)$ negative and $\psi(z_c)$ postive. Their failure to include points z_b, z_c, z_d in the figure make it difficult to interpret this result.

The contributions of the fifth and higher order terms must be evaluated to ensure that the elimination of the third order terms

does not simply shift the nonlinearities to higher order. The complete evaluation of there higher order terms, which is a complicated numerical problem, is required before one can be assured of meeting design requirements.

Collective Particle Optics

4.1 Introduction

In the previous section the motion of a single charged particle in an external magnetic field was described. The motion of a charged particle in the electric field produced by the other charged particles of the beam will now be considered. In electromagnetic theory, free charges in the region of the calculation are treated individually as either point charges or collectively using a charge density ρ. The electric fields produced by external charges and from the space charges are added vectorally. To study the effect of the Coulomb interactions on the motion of particles, it is necessary to assume a particle (charge) distribution, one that seems appropriate to the actual problem and for which a solution can be obtained. The appropriateness of the charge distribution must be verified experimentally. The lack of knowledge of the actual distribution and the limited number of charge distributions for which solutions can be obtained make space charge calculations difficult. Soon, we will describe the calculations by E. Colton, Ref. [4], of space-charge and third-order aberrations in a quadrupole focusing system. It should be emphasized that these calculations use two very simple charge distributions. The calculations produce analytic expressions that show space charge and third order aberration effects, but they may not be useful in predicting the space charge effect in actual systems in which the charge distribution differ. In particular, he does not solve the problem for a Gaussian distributed beam which is frequently used as

representative of an actual beam because in his words "the mathematical treatment is difficult."

Ideally one would like to determine the time evolution of the charge distribution as the beam propagates along the transport system. However, it is a complicated many body problem. The evolution of the charge distribution will most likely depend critically on the set of initial conditions for all the beam particles, i.e., depends on the phase space of the beam. The very large number of particles in a beam makes it impossible to track all the particles through the system while they undergo Coulomb interactions. It is possible to do simulations using a reduced number of particles, by concentrating charge on larger particles. However, this macro particle method has computational difficulties when the macro particles approach one another too closely. To obtain convergent results their motion must be restricted. How this restriction is made directly affects the result of the calculations.

Since the many particle problem is so difficult, one must resort to single particle calculations in the effective electric field of the beam. Ordinarily, the charge distribution will not remain constant. There are two approaches that can be used to treat this problem consistently. In the first the initial distribution is specified and the particle trajectories are calculated and the temporal variation of the charge distribution is calculated. In the second, a stationary charge distribution is assumed and the particle trajectories are calculated and shown to be consistent with it.

4.2 Space Charge and Aberrations in Quadrupole Systems

To demonstrate how the space charge effect can be introduced into the single particle optics, a sample calculation will be presented. It is based on a paper by E.P. Colton, "Space-Charge and Third-Order Aberrations in Quadrupole Focusing Systems", Ref. [4]. What follows is based on this paper. The reader is referred to it for a more detailed discussion. (The paper is not long.)

Throughout the NPB device quadrupoles are used to focus the beam. Bends and telescopes use quadrupole focusing, so this particular treatment of space-charge and third order aberrations in quadrupole focusing systems is appropriate. Colton derives a set of equations (x and y) for the transverse oscillations in electric and magnetic fields caused by space charge and magnetic fields of quadrupoles and octupoles. The third-order aberrations of a point-to-parallel system are calculated. A point to parallel system in design so all particles passing through a designated point will emerge from the system with x' = 0. Two transverse charge densities are used, uniform and parabolic.

The equations of motion for a single charge particle are obtained from the Lorentz force

$$\vec{F} = e (\vec{E} + \vec{v} \times \vec{B}) \tag{4.1}$$

where $\vec{E}$, $\vec{v}$ and $\vec{B}$ are the usual vector quantities and e is the electric charge. To obtain the equations of motion in cartesian coordinates (x,y,s), we define the radius vector

$$\vec{r} = x\hat{i} + y\hat{j} + s\hat{k} \tag{4.2}$$

89

$$\vec{v} = \dot{x}\hat{i} + \dot{y}\hat{j} + \dot{s}\hat{k}$$

and

$$\dot{\vec{v}} = \ddot{\vec{r}} = \ddot{x}\hat{i} + \ddot{y}\hat{j} + \ddot{s}\hat{k}$$

where $\hat{i}$, $\hat{j}$, $\hat{k}$ are the unit vectors in the x, y and s directions. The equations of motion obtained from Eq. (4.1) are

$$\ddot{x} = \frac{e}{m}(\dot{y}B_s - \dot{s}B_y)$$
$$\ddot{y} = \frac{e}{m}(\dot{s}B_x - \dot{x}B_s) \qquad (4.3)$$
$$\ddot{s} = \frac{e}{m}(\dot{x}B_y - \dot{y}B_x)$$

where m is the relativistic mass. To convert from time t to the path distance s, as the independent variable, we use the following relationships

$$\dot{x} = x'\dot{s}$$
$$\qquad (4.4)$$
$$\ddot{x} = x''\dot{s}^2 + x'\ddot{s}$$

with

$$v^2 = \dot{s}^2 + \dot{x}^2 + \dot{y}^2 \qquad \text{and}$$
$$\qquad (4.5)$$
$$\frac{1}{\dot{s}} = \frac{1}{v}(1 + x'^2 + y'^2)^{1/2}$$

Substitution of the third equation of Eq.(4.3) into the first two gives the following equations for x and y.

$$x'' = \frac{e}{p}T'\left(T'\frac{E_x}{v\gamma^2} + y'B_s - (1 + x'^2)B_y + x'y'B_x\right) \qquad (4.6a)$$

and

$$y'' = -\frac{e}{p}T'\left(-T'\frac{E_y}{v\gamma^2} + x'B_x - (1 + y'^2)B_y + x'y'B_y\right) \qquad (4.6b)$$

where $T' = \sqrt{1+x'^2+y'^2}$. The primes on x and y denote derivatives with respect to s or z as was the case in Section 3. For these equations the defocusing of the space-charge field E and the azimuthal magnetic field are combined into a net electric field which reduces the electric field by a factor $1/\gamma^2$. The expression for the components of the electric field can be obtained from the equation

$$E = -\nabla\phi \qquad (4.7)$$

where ϕ is the electrostatic potential. The ϕ is obtained by solving the Poisson equation

$$\nabla^2\phi = -\rho(x,y)/\varepsilon_o \qquad (4.8)$$

where $\rho(x,y)$ is the charge density distribution. Colton solved the problem for two charge density distributions. He assumed the beam to be an ellipsoid in x-y space

$$\left(\frac{x}{a}\right)^2 + \left(\frac{y}{b}\right)^2 = 1 \qquad (4.9)$$

One distribution was for a uniformly populated ellipsoid with longitudinal density $\lambda(s)$

$$\rho(x,y) = \rho_0 = \frac{\lambda(s)}{\pi ab} \tag{4.10}$$

and the second has a parabolic distribution

$$\rho(x,y) = 2\rho_0 [1 - (\frac{x}{a})^2 - (\frac{y}{b})^2] \quad . \tag{4.11}$$

The corresponding expressions for $\phi(x,y,s)$ for the two cases solving Eq. (4.4) are

$$\phi(x,y,s) = -\rho_0 \frac{e(bx^2 + ay^2)}{2\varepsilon_0(a + b)} \tag{4.12}$$

and

$$\phi(x,y,s) = -\frac{\rho_0 eab}{2\varepsilon_0(a + b)} (\frac{2x^2}{a} + \frac{2y^2}{b} - \frac{(2a + b)x^4}{3a^3(a + b)}$$
$$- \frac{2x^2 y^2}{ab(a + b)} - \frac{(a + 2b)y^4}{3b^3(a + b)}) \tag{4.13}$$

He claims that these charge distributions are self-consistent and do not produce emittance growth.

The equation of motion can be written

$$x'' = \frac{e}{p} (\frac{E_x^L m_0}{p\gamma} - gx) \tag{4.14a}$$

and

$$y'' = \frac{e}{p} (\frac{E_y^L m_0}{p\gamma} + gy) \tag{4.14b}$$

when the right-hand sides of Eq. (4.6) are expanded to first order in the displacement (x or y) or their derivatives (x' or y'). This is the paraxial approximation ($x'^2 \ll 1, y'^2 \ll 1$ and $x'y' \ll 1$). The longitudinal magnetic fields B_s are quadratic in the coordinates and can therefore be ignored. The g in Eq. (4.14) is the quadrupole gradient

$$g = \frac{\partial B_y}{\partial x} \Big|_{x=y=0} \ .$$ (4.15)

The E^L represents the electric field in the linear approximation. After calculating the electric fields, Eqs. (4.14a and b) can be written

$$x'' + (k - \alpha k_{sx})x = 0$$ (4.16a)

and

$$y'' - (k + \alpha k_{sy})y = 0$$ (4.16b)

where $k = eg/p$, and

$$k_{sx} = \frac{e m_o \rho_o eb}{p^2 \gamma \varepsilon_o (a + b)}$$ (4.17a)

and

$$k_{sy} = a k_{sx}/b \ .$$ (4.17b)

For the uniform distribution $\alpha = 1$ and for the parabolic distribution $\alpha = 2$.

The envelope equations, Eq. (2.69), are obtained from Eqs. (4.16a and 4.16b),

$$a'' + (k - \alpha k_{sx}) a - \frac{\epsilon^2}{a^3} = 0 \qquad\qquad (4.18a)$$

and

$$b'' - (k + \alpha k_{sy}) b - \frac{\epsilon^2}{b^3} = 0 \qquad\qquad (4.18b)$$

where ϵ is the transverse beam emittance. Colton claims that this first order treatment is self-consistent since

(1) Eqs. (4.18) are used to obtain a and b in order to specify k_{sx} and k_{sy}'s; and

(2) single particles are then propagated using Eqs. (4.16).

Now we are ready to look at the third order terms. The quadrupole fields through third order can be written

$$B_x = y(g - g''/12 \ (3x^2 + y^2)) \qquad\qquad (4.19a)$$

$$B_y = x(g - g''/12 \ (x^2 + 3y^2)) \qquad\qquad (4.19b)$$

and

$$B_s = xyg' \qquad\qquad (4.19c)$$

The equations of motion Eqs. (4.6) can be written (following the notation of Colton)

$$x" + (k - \alpha k_{sx})x = (D_1 - k)xx'^2 + D_1 xy'^2 + kx'yy'$$

$$(4.20a)$$

$$+ k'xyy' + (x^3/3)D_2 + xy^2 D_3$$

and

$$y" - (k + \alpha k_{sy})y = (E_1 + k)yy'^2 + E_1 x'^2 y - kxx'y'$$

$$(4.20b)$$

$$- k'xx'y - (y^3/3)E_2 - x^2y E_3$$

where the D and E functions are defined as

$$D_1 \equiv \alpha k_{sx} - k/2 \qquad (4.21a)$$

$$E_1 \equiv \alpha k_{sy} + k/2 \qquad (4.21b)$$

$$D_2 \equiv \frac{k"}{4} - \frac{\alpha(\alpha - 1) k_{sx}(2a + b)}{a^2(a + b)} \qquad (4.21c)$$

$$E_2 \equiv \frac{k"}{4} + \frac{\alpha(\alpha - 1) k_{sy}(a + 2b)}{b^2(a + b)} \qquad (4.21d)$$

$$D_3 \equiv \frac{k"}{4} - \frac{\alpha(\alpha - 1) k_{sx}}{b(a + b)} \qquad (4.21e)$$

and

$$E_3 \equiv \frac{k"}{4} + \frac{\alpha(\alpha - 1) k_{sy}}{a(a + b)} \qquad (4.21f)$$

To include octupole lens (hard edged) the coefficient of the cubic terms x^3, xy^2, y^3 and x^2y are replaced. Thus $D_2 \rightarrow D_2 - 3W$, $E_2 \rightarrow E_2 + 3W$, $D_3 \rightarrow D_3 + 3W$ and $E_3 \rightarrow E_3 - 3W$ where $W = eB'''/p$ and $B''' = \partial^3 B_y/\partial x^3$ at $x = y = 0$.

Particles can be tracked through the transport line using Eqs.(4.20) for the uniform distribution. For the parabolic charge distribution a multiparticle simulation is required to obtain a self-consistent result.

Colton, at this point, indicates that the quadrupole edges represents a major contribution to third order effects, and that high order terms in $k(k',k'')$ can be replaced with higher order x and y factors.

Usually the contributions of the higher order terms are of particular interest since they contribute to the spot size or the divergence of the beam. By using the matrix method, as described in section 2 and used in section 3, and the Green's function integration, a standard method of solving differential equations in which the nonlinear terms are treated as driving terms (described in Section 3), he obtains the small angular error terms to the third order for a point-to-parallel transformation.

$$\Delta x'_f = (x'_f | x'^3_o) \ x'^3_o + (x'_f | x'_o y'^2_o) \ x'_o y'^2_o \tag{4.22a}$$

and

$$\Delta y'_f = (y'_f | x'^2_o \ y'_o) \ x'^2_o y'_o + (y'_f | y'^3_o) \ y'^3_o \tag{4.22b}$$

By ignoring the effects of space charge and octupoles ($k_{sx} = k_{sy} = 0$) initially, and integrating by parts to remove k' and k'', the coefficients are given by

$$(x'_f | x'^3_o) = C'_x \ (s_f) \int_o^{s_f} (\frac{k}{2} \ S^2_x S'^2_x + k^2 \ \frac{S^4_x}{3}) \ d\sigma \tag{4.23a}$$

96

$$(x_f'|x_o'y_o'^2) = - C_x' (s_f) \int_o^{s_f} [k(S_x S_x' S_y S_y' + \frac{S_x'^2 S_y^2}{2} - S_x^2 S_y'^2)$$

$$- S_x^2 S_y^2 k^2] \, d\sigma \qquad (4.23b)$$

$$(y_f'|x_o'^2 y_o') = C_y' (s_f) \int_o^{s_f} [k(S_x S_x' S_y S_y' + \frac{S_x^2 S_y^2}{2} - S_x'^2 S_y^2)$$

$$- S_x^2 S_y^2 k^2] \, d\sigma \qquad (4.23c)$$

and

$$(y_f'|y_o'^3) = C_y' (s_f) \int_o^{s_f} (- \frac{k}{2} S_y^2 S_y'^2 + \frac{S_y^4}{3} k^2) \, d\sigma \qquad (4.23d)$$

where C's and S's are as defined in Eq.(3.14). I recognize that thse expressions are complicated.

The final step, to include space charge and octupoles, is to replace k^2 of (4.23a,b,c, and d) respectively with

$$k^2 \rightarrow k^2 + \frac{\alpha(\alpha - 1)k_{sx}(2a + b)}{a^2(a + b)} + 3W \qquad (4.24a)$$

$$k^2 \rightarrow k^2 + \frac{\alpha(\alpha - 1)k_{sx}}{a(a + b)} - 3W \qquad (4.24b)$$

$$k^2 \rightarrow k^2 + \frac{\alpha(\alpha - 1)k_{sy}}{a\ (a + b)} - 3W \qquad (4.24c)$$

$$k^2 \rightarrow k^2 + \frac{\alpha(\alpha - 1)k_{sy}(a + 2b)}{b^2(a + b)} + 3W \qquad (4.24d)$$

The contribution of these higher order aberrations on the divergence of the beam. Eqs. (4.23) and (4.24) can be reduced by adjusting the octupoles of the system.

4.3 Achromatic Bend with Space Charge

An achromatic bend is a beam transport device used to change the direction of propagation of a beam. As shown in Fig. 31, it consists of a sequence of dipoles and quadrupoles placed along the bending arc.
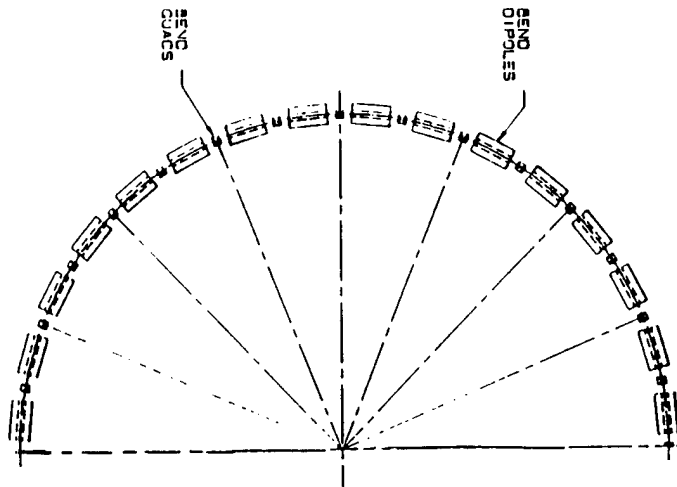
Figure 31. An achromatic bend

The magnetic field of the dipoles change the beam direction and the quadrupoles focus the beam in the transverse direction. The term achromatic means the dispersion (ℓ), the spread of the

98

beam in the direction of propagation, and the momentum spread (δ = $\Delta p/p$) do not change as a result of the beams passing through the device. To first order, the achromatic condition is satisfied for a lattice of identical cells if and only if

1) $M^n = I$

and
$$(4.25)$$

2) $\ell = 0$ and $\delta = 0$. (no dispersion or momentum spread)

where M is the transfer matrix for the transverse direction, for each lattice cell. A first order achromat has a total transfer matrix which is the identity matrix (I). The total phase advance must be a multiple of 2π ($2m\pi$ where m is an integer). A second order achromat is one whose total transfer matrix is the identity matrix to second order of all phase space variables except the matrix element relating the path length ℓ to the square of δ. A 180° bend such as that shown in Fig. 31, is designed to have a phase advance of 720° or 90° for each section.

The design of an achromatic bend, in which the effects of space charge are ignored, can be done using the available techniques. The difficulty arises when space charge effects dominate. In those cases, there is usually a distinction made between systems in which the space charge can be approximated using a linear self-field and those in which the nonlinearities are important. In Ref. [10], Jason et al site the work of Sacherer who "showed that motion of the rms envelope is independent of the beam distribution; hence, core evolution can be described by a linear model," as support for their claim that a linear approximation has

99

some validity. Also they site the work of Hofmann, "who noted that focused beams tend to evolve toward uniform spatial distribution if the nonlinearities are not such as to provoke instability." They use the linear approximation to obtain the analytic results presented in Ref. [10].

They observe that even in the linear space charge case the longitudinal motion evolves in a quasi irreversible manner and couples to the transverse motion. This occurs in the dispersive case such as in bending magnets. They give the following argument to illustrate this point. The transformation through $d\ell$, an infinitesimal length in a bend magnet, can be written (ignoring motion in the y-y' plane)

$$
\begin{vmatrix}
B_{11} & B_{12} & 0 & B_{16} \\
B_{21} & B_{22} & 0 & B_{26} \\
B_{51} & B_{52} & 1 & B_{56} \\
0 & 0 & 0 & 1
\end{vmatrix}
\times
\begin{vmatrix}
1 & 0 & 0 & 0 \\
\lambda_x d\ell & 1 & 0 & 0 \\
0 & 0 & 1 & 0 \\
0 & 0 & \lambda_z d\ell & 1
\end{vmatrix}
\tag{4.26}
$$

where the left matrix is the transformation for a magnet of length $d\ell$ and the right matrix is the space charge kick with transverse and longitudinal defocusing gradients λ_x and λ_z. The separation into two separate parts is one way of calculting the linear space charge numerically. They indicate that the presence of the $\lambda_z d\ell$ element is responsible for mixing the motion in the transverse

and longitudinal directions. For illustration the generic form
for the result was written

$$
\begin{vmatrix}
R_{11} & R_{12} & R_{15} & R_{16} \\
R_{21} & R_{22} & R_{25} & R_{26} \\
R_{51} & R_{52} & R_{55} & R_{56} \\
R_{61} & R_{62} & R_{65} & R_{66}
\end{vmatrix}
\qquad (4.27)
$$

For a nondispersive system, even with space charge, the elements
R_{15}, R_{25}, R_{61} and R_{62} would be zero. For the dispersive case they
are non-zero. This result depends only on the space charge forces
being linear in $d\ell$.

For the zero current case, the independence of motion in the
transverse plane from the longitudinal motion, the achromatic
condition, is satisfied when $R_{16} = R_{26} = 0$. They show that this
is not sufficient when space charge is present. By using a
sequence of transformations, R^0, R^1 and R^2, in which R^1 contains
dispersive elements, the other two do not, the R^t_{16} and R^t_{26}
elements of the total transfer matrix R^t ($= R^2 \cdot R^1 \cdot R^0$) can be
written

$$
R^t_{16} = R^2_{11}(R^1_{15}R^0_{56} + R^1_{16}R^0_{66}) + R^2_{12}(R^1_{25}R^0_{56} + R^1_{26}R^0_{66})
$$

and $\qquad (4.28)$

$$
R^t_{26} = R^2_{21}(R^1_{15}R^0_{56} + R^1_{16}R^0_{66}) + R^2_{22}(R^1_{25}R^0_{56} + R^1_{26}R^0_{66})
$$

For R^t_{16} and R^t_{26} to be zero the elements R^l_{15} and R^l_{25} must also be zero. For the dispersive case the achromatic conditions to first order is satisfied when $R_{16} = R_{26} = R_{15} = R_{25} = 0$. They also show that under this transformation, R^t, the transverse emittance remains constant where these matrix elements are zero.

Their main observation was that if one is designing a achromatic bend assuming linear space charge that these four matrix elements must be adjusted to zero for each section.

Their work does not justify the assumption of linear space charge. Given the difficulties of the nonlinear space charge case, much additional analytic numerical and experimental work is required to demonstrate that an achromatic bend can be designed for the high current case.

4.4 Scaling Relations

This brings us to the last topic on space charge, the work of E. A. Wadlinger on scaling relations, Ref. [11]. Scaling has been used for modeling of physical problems for many years. The most obvious example is the modeling of the flow of fluids around actual full size objects, such as boats and planes with the flow around scale models of these objects in wind tunnels and tow tanks. Even for these very nonlinear systems, the results will be identical if the scaling is done properly. This approach has proven to be a time and money-saver.

This same technique has been applied to the motion of a particle in a charged particle beam with space charge. Wadlinger has demonstrated that the equations of motion for two different nonrelativisitic beams, with time dependent (or independent)

102

electric and magnetic external fields and with space charge are identical if parameters of the two beams satisfy a set of scaling relations. For this case, the length, time, beam current, electric pole tip fields, magnetic pole tip fields and the normalized emittance are scaled quantities. He assumes that the internal and external electric and magnetic fields can be expressed using multipole expansions. This assumption is the one cited by those who question the validity of his approach, since the Coulomb fields of the beam particles cannot be expanded in this way.

If this procedure is correct, then results obtained on one machine could be used to predict the beam dynamics on another, or the knowledge of the dynamics for one set of beam parameters could be used to predict the dynamics for another set of parameters on the same machine!

REFERENCES

1. Stanley Humphries, Jr., <u>Principles of Charged Particle Acceleration</u>, John Wiley & Sons, New York, 1986.

2. Karl L. Brown and Roger V. Servranckx, "First-and Second-Order Charged Particle Optics", Physics of High Energy Particle Accelerators, AIP Conference Proceedings, No. 127, Editors M. Month, P. Dahl and M. Dienes, American Institute of Physics, New York 1985, pages 64-138.

3. Klaus G. Steffen, <u>High Energy Beam Optics</u>, Interscience Publishers, a division of John Wiley & Sons, New York, 1965.

4. Eugene P. Colton, "Space-Charge and third-order aberrations in quadrupole focusing systems", Proceedings of the Second International Conference on Charge Particle Optics, Albuquerque, May 19-23, 1986, Editors S.O. Schriber and L.S. Taylor, North-Holland-Armsterdam, 1987, pages 566-571.

5. J.D. Lawson, "Space Charge Optics", Advances in Electronics and Electron Physics, Supplement 13c. Academic Press, Inc., 1983, pages 1-48.

6. I. Hofmann, "Transport and Focusing of High-Intensity Unneutralized Beams", Advances in Electronics and Electron Physics, Supplement 13c. Academic Press, Inc. 1983, pages 49-140.

7. D.A. Edwards, "An Introduction to Circular Accelerators", Physics of High Energy Particle Accelerators, AIP Conference Proceedings, No. 127, Edited by M. Month, P. Dahl and M. Dienes, American Institute of Physics, New York, 1985, page 1-61.

8. R.W. Moses, E.A. Heighway, R.S. Christian, and A.J. Dragt, "Scaling Laws for Aberrations in Magnetic Quadrupole Lens Systems," Los Alamos National Laboratory, National Laboratory report (LA-UR-87-297-Revised), submitted to the 1987 Particle Accelerator Conference, March 16-19, 1987, Washington, DC.

9. R. Moses, "Quadrupole-Octupole Aberration Correctors with minimum Fields," Rev. Sci. Instr., Vol. 42, pp. 832-839, 1971.

10. A.J. Jason, E.M. Svaton, B. Blind, and E.A. Heighway, "Design of Achromatic Bending Systems in the Presence of Space Charge," Los Alamos National Laboratory report LA-UR-87-778, submitted to the 1987 Particle Accelerator Conference, Washington, DC., March 16-19, 1987.

REFERENCES (Cont'd)

11. E.A. Wadlinger, "Beam-Transport Channel Scaling to Produce Different but Equivalent Transport Systems," Workshop on Linear Accelerator and Beam Optics Codes, San Diego, CA, January 1988.

12. Claude Lejeune and Jean Aubert, "Emittance and Brightness: Definitions and Measurements," Advances in Electronics and Electron Physics, Supplement 12A, Academic Press, 1980.

13. A.J. Lichtenberg, "Phase Space Dynamics of Particles", Wiley, New York, 1969.

14. P. Lapostolle, "Quelques effets essentiels de la charge d'espace dans les faisceaux continus," Rep. CERN/DI-70-36 (1970).

15. John Farrell, Private communication, 1987.

Assume 5×10^{17} p/s, 3mm dia, 10^8 N/s

$\pi r^2 \approx 7 \, mm^2 \qquad = 10^{10} \, cm/s$

$= 7 \times 10^{-2} \, cm^2$

$\dfrac{5 \times 10^{17}}{7 \times 10^8} \approx 1 \times 10^9 \, p/cm^3$

particle density in accelerator $10^9 - 10^{10}$ p/cm^3

$E = \int \bar{F} \cdot d\bar{r} = \int_0^x kx \, dx = \frac{1}{2} kx^2$

① How much — or how many pieces — of our generic beam control apparatus has been built & tested? Compactor? Bend — or any portion thereof. Octupole/Sextupole correctors?